Ore Geology Reviews 88 (2017) 201–234

Contents lists available at ScienceDirect

Ore Geology Reviews

journal homepage: www.elsevier.com/locate/oregeo

Review

Paleovalley-related uranium deposits in Australia and China: A review of geological and exploration models and methods

Baohong Hou [a,*], John Keeling [a], Ziying Li [b]

[a] Geological Survey of South Australia, GPO Box 1671, SA 5000, Australia
[b] Beijing Research Institute of Uranium Geology (BRIUG), CNNC, Beijing, PR China

ARTICLE INFO

Article history:
Received 6 February 2017
Received in revised form 1 May 2017
Accepted 3 May 2017
Available online 6 May 2017

Keywords:
Paleovalley
Uranium
Geology
Exploration
Models and methods
Australia
China

ABSTRACT

The features and similarities in the geology of paleovalley-related uranium mineralizing systems in Australia and China can be used to refine strategies for exploration. Paleovalley-related uranium resources include sandstone-, lignite- and calcrete-style deposits that are developed within the host sediments deposited in paleovalleys. The paleovalleys incise either crystalline bedrock or older sedimentary rocks, and uranium was deposited and concentrated by the influx of oxidized/reduced groundwaters flowing in aquifers within the paleovalley fill. The critical features of paleovalley-related uranium deposits include sediment and uranium sources, geological setting, depositional environment, age and relative timing of mineralization, aquifer characteristics, availability and distribution of reductants, and preservation potential of the uranium mineral system. This set of information provides a basis to establish the uranium mineralization model, which can then be used to assist with generating targets for uranium exploration and prospectivity analysis of a region. With respect to Sino-Australian examples, paleovalley-related uranium deposits form mostly around the margins of sedimentary basins and the mineralization is commonly hosted within channel fills contained within paleovalleys developed upon, or proximal to, Precambrian crystalline rocks that contain primary uranium sources. The deposits that have been well studied show remarkably similar factors that controlled the formation of paleovalley-related uranium deposits. Basement/bedrocks with above-background (2.8 ppm U) levels of uranium (10–100 ppm) that are linked to, and/or, incised by paleovalleys are associated with these deposits and are the inferred source of the uranium. In these regions, extensive fluvial systems developed particularly during Mesozoic and Cenozoic times, uranium from the bedrock was first dispersed into the sediments, and then concentrated to form deposits through successive chemical remobilization, precipitation and concentration. The deposits formed in continental or marginal marine environments, and commonly are associated with reduced lithologies, containing pyrite and dispersed organic matter and/or seams of lignite, or show evidence of infiltrated hydrocarbons. The mineralization is developed where oxidizing fluids (carrying dissolved U) reacted with reductants in the sediments. Geological, geophysical and geochemical features of the paleovalleys and related uranium deposits are used to construct models to understand host sediment distribution, fluid flow and ore genesis that can assist exploration for paleovalley-hosted uranium deposits. Precise geometric definition of the basin margin and paleovalley architecture is important in identifying exploration targets and improving the effectiveness of drilling. Refinements in remote sensing, geophysical and data processing techniques, in combination with sedimentological and depositional interpretations, provide an efficient approach for outlining the principal drainage patterns and channel dimensions. To help reduce risk, an exploration strategy should combine these technologies with a detailed understanding of the physicochemical parameters controlling uranium mobilization, precipitation and preservation.

© 2017 Elsevier B.V. All rights reserved.

* Corresponding author.

http://dx.doi.org/10.1016/j.oregeorev.2017.05.005
0169-1368/© 2017 Elsevier B.V. All rights reserved.

Contents

1. Introduction . . . 202
2. Paleovalley-related uranium mineral systems . . . 205
2.1. Source rocks. . . . 205
2.2. Geological setting . . . 207
2.3. Mineralization and preservation . . . 208
2.4. Sandstone-hosted uranium deposits . . . 210
2.4.1. Carnarvon, Canning, Amadeus and Ngalia basins, Australia . . . 211
2.4.2. Callabonna Sub-basin of the Lake Eyre Basin, South Australia . . . 212
2.4.3. Eucla Basin, Australia . . . 213
2.4.4. Pirie Basin, South Australia . . . 215
2.4.5. Ordos Basin, north China . . . 215
2.4.6. Songliao Basin, northeast China. . . . 219
2.4.7. Erlian Basin, north China . . . 219
2.4.8. Yili and Tuha Basins, northwest China . . . 223
2.5. Lignite-hosted deposits . . . 223
2.6. Calcrete-hosted (surficial) deposits . . . 225
2.6.1. Calcrete-uranium in Australia . . . 226
3. Geological models . . . 226
4. Exploration methodology. . . . 228
4.1. Paleovalley mapping . . . 228
4.1.1. Remote sensing imagery . . . 228
4.1.2. Geophysical methods . . . 228
4.1.3. Structural and basement geology . . . 229
4.1.4. Sedimentological analysis . . . 229
4.1.5. 3D modelling . . . 229
4.2. Location, definition and assessment of mineralization . . . 229
5. Discussion and conclusions . . . 229
5.1. Reductants . . . 229
5.2. Source of uranium. . . . 230
5.3. Implications for sandstone-hosted or lignite-hosted deposits . . . 230
6. Conclusions. . . . 230
Acknowledgements . . . 231
References . . . 231

1. Introduction

Exploitable uranium resources are found in diverse geological settings (e.g., igneous, hydrothermal and sedimentary environments) and the various deposits have been broadly subdivided into 14 categories based on the host-rock type and geological setting (OECD/NEA and IAEA, 2000). The various categories of uranium deposits in Australia (Fig. 1) and China (Fig. 2) and their relative economic significance, compared with worldwide resources, are summarized in Table 1. Categories of uranium deposit included here as paleovalley-related uranium mineral systems, are the sandstone-, lignite- and calcrete-hosted uranium deposits formed during various depositional (sedimentation) and post-depositional (diagenesis and post-sedimentation fluid-flow) stages of basin and/or paleovalley evolution; these deposits represent a significant portion (>25%) of worldwide known uranium resources (IAEA, 2009). Paleovalley-related uranium deposits are the major source of uranium across the Central-Asia Uraniferous Province (CAUP, including southern Russia, southern Kazakhstan, Uzbekistan, Mongolia and north China; OECD-NEA/IAEA, 2010) and large deposits are located in central and southwestern Australia. Major uranium resources of similar style also occur in USA, Niger, Gabon (Franceville Basin), and South Africa (Karoo Basin). Worldwide, paleovalley-related sediments have provided and will continue to provide uranium from medium-grade deposits at relatively low cost (McKay and Miezitis, 2001). For many deposits of this style, the uranium is concentrated within sediments deposited in fluvio-deltaic paralic environments (Fig. 3). The development of ore-grade uranium is influenced by various factors including sediment permeability, presence of reductant (e.g., organic matter), proximity to uranium bedrock source regions, and favorable groundwater flow. Both Australia and China currently have significant undeveloped resources in paleovalley-related uranium deposits and ongoing exploration continues to make new discoveries.

Global exploration for paleovalley-related uranium deposits is focused mostly on Mesozoic and Cenozoic sediments adjacent to Archean-Proterozoic cratons containing uranium-enriched igneous rocks, such as the Gawler and Curnamona Provinces in South Australia, Yilgarn Craton in Western Australia (Fig. 1) (Curtis et al., 1990) and northern China Platform and cratons in the Qilian-Qinling and Tianshan Provinces of China (Fig. 2; Zhang and Li, 2008). Mesozoic sedimentary basins of north China located at the southeastern edge of the CAUP are highly prospective for uranium, with ongoing discovery of ore deposits that are amenable to uranium extraction by *in situ* leach techniques (ISR). Over 50% of currently identified uranium resources in China are contained within sandstone-hosted deposits, as roll front and tabular-shaped ore bodies in the Mesozoic sedimentary basins of north China (OECD-NEA/IAEA, 2014). Renewed interest in uranium exploration, in Australia and China post-2005, was directed largely towards drilling Cenozoic and Mesozoic sediments, including paleovalley sediments in South Australia and Western Australia (e.g., Callabonna Sub-basin, Eucla Basin, Gawler and Yilgarn cratons) and north China (e.g., Yili, Erlian, Ordos and Songliao basins).

This review paper presents an overview of the three important types of paleovalley-related uranium systems in Australia and China, with an outline of the geology and characteristics of the deposits and exploration approaches that can assist in identifying prospective targets at regional and local scales. The conceptual

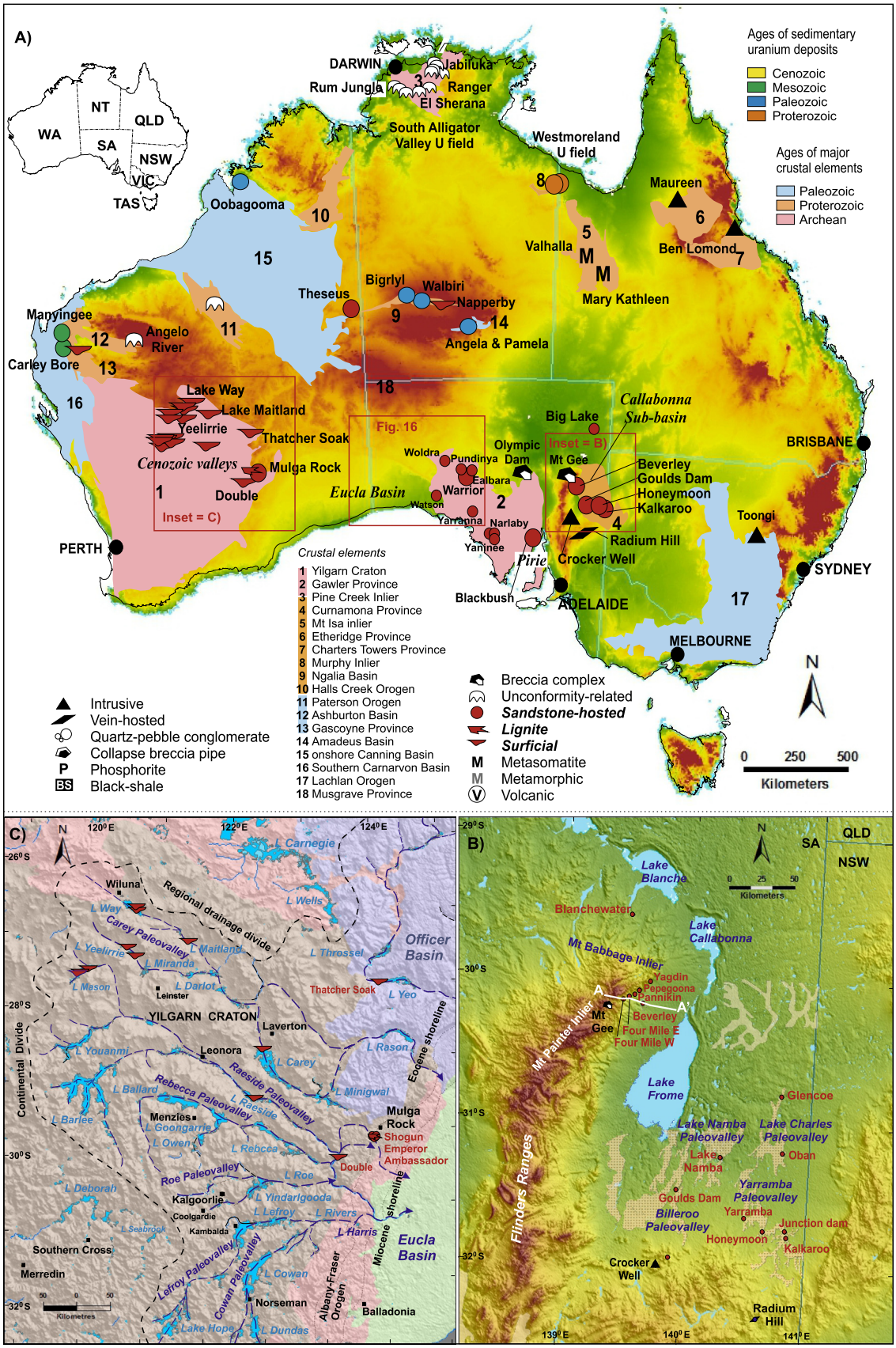

Fig. 1. A): Main uranium deposits/metallogenic and source regions in Australia (data sourced from Australia's OZMIN dataset 2014); B) major paleovalleys and related uranium deposits in Callabonna Sub-basin of South Australia; C) major Eucla paleovalleys and related uranium deposits in Yigarn Craton and western Eucla Basin (modified from de Broekert, 2002; Hou et al., 2008).

Fig. 2. A) Main uranium deposits/metallogenic regions in China (after Zhang and Li, 2008; Hou et al., 2014); B) major highlands and U-bearing sedimentary basins in north China (the image is from CNNC).

Table 1
Types of uranium deposits. Numbers represent the approximate economic Australia significance of the seven most important deposit types while numbers in brackets represent the approximate economic worldwide significance of the seven most important deposit types (from McKay and Miezitis, 2001; OECD/NEA and IAEA, 2012; Zhang and Li, 2008).

Types of uranium deposits	Ranking of importance (contained U_3O_8) with respect to country		
	Australia	China	Worldwide*
Breccia complex deposits (3)	1		2
Unconformity-related deposits (1)	2		3
Sandstone deposits (2)	3	1	1
Surficial deposits (6)	4		6
Metasomatite deposits (7)	5	5	7
Metamorphic deposits	6		
Volcanic deposits	7	3	
Intrusive deposits (5)	8	6	5
Vein deposits	9	2	
Quartz-pebble conglomerate deposits (4)	10	–	4
Collapse breccia pipe deposits	11	–	
Phosphorite deposits	12	8	
Lignite	13	7	
Black shale deposits	14	4	

* 7 major uranium resources worldwide. ***Paleovalley-hosted uranium deposit types in bold italic.***

models and key exploration criteria for paleovalley-related uranium systems, derived from Australian and Chinese examples, have broader application in similar settings worldwide.

2. Paleovalley-related uranium mineral systems

In the context of this paper, 'paleovalley-related' uranium systems encompass variants of 'sandstone-hosted' deposits, lignite-type deposits, and surficial deposits of the 'calcrete' type developed within fluvio-lacustrine sediments (Table 2). Examination of the known paleovalley-related uranium deposits worldwide show that such uranium deposits mostly occur either in paleovalleys that incised weathered bedrock (e.g., Gawler and Yilgarn cratons, Australia) or sedimentary deposits on the margins of sedimentary basins during lowstands in the low-relief regions (e.g., Callabonna Sub-basin and Eucla Basin of Australia; Yili, Erlian, Ordos and Songliao basins of China), including paleovalley-related alluvial fans developed in the high-relief areas (e.g., Dalmatov uranium deposit of Russian, Dai, 1996; Four Mile deposits along the northwestern margin of the Callabonna Sub-basin, see below).

2.1. Source rocks

The distribution of known sedimentary uranium resources shows a clear spatial relationship with uranium-enriched bedrock in Australia (Lambert et al., 2005) and China (Zhang and Li, 2008). The location of deposits is strongly influenced by the presence of uranium-rich source rocks in the headwaters of paleovalleys draining into sedimentary basins developed in Australia (particularly in Northern Territory, Western Australia and South Australia) and China (e.g., Tianshan region, Ordos, Erlian, and Songliao Basin, northern China). The uranium released by weathering of rocks in the source areas is mobilized either in surface and ground waters or physically transported and incorporated as detritus in the sedimentary deposits, to be subsequently leached and remobilized within the sediment.

In Australia, significant uraniferous igneous rocks (containing >10 ppm uranium) formed during the Proterozoic and are widespread throughout South Australia, the Northern Territory, Western Australia and parts of Queensland. In South Australia, the distribution of anomalously high uranium-bearing granites in the region of the Callabonna Sub-basin are correlated also with areas of high geothermal gradient in the basin sediments with minor hot springs due to radiogenic heat from the granitic bedrock (Brugger et al., 2005; Lambert et al., 2005). Paleovalley-related uranium deposits within the Callabonna Sub-basin of South Australia occur proximal to highlands of Proterozoic rock containing significant uranium enrichment (e.g., the Mount Painter Inlier, Curnamona Province) (Ludwig and Cooper, 1984; Elburg et al., 2001; Hou et al., 2006; Fraser and Neumann, 2010; Jagodzinski and Fricke, 2010; Wade, 2011). The average uranium content in the bedrock varies between 4 and 100 ppm, although some felsic rocks in the Mount Painter and Mount Babbage inliers contain up to ~400 ppm uranium (Jaireth et al., 2015). The Honeymoon Granite, which is spatially associated with the Honeymoon and East Kalkaroo uranium deposits, contains up to 40 ppm uranium. The Honeymoon Granite shows locally intensive potassic alteration (Fricke and Reid, 2009). Unaltered Honeymoon Granite has an abundance of uranium-bearing minerals (uranium oxides in pyrite, monazite, allanite, zircon and apatite). The felsic rocks in the Olary Domain, to the south of the Callabonna Sub-basin, contain several orthomagmatic and hydrothermal uranium deposits (e.g., Crocker Well, Mount Victoria and Radium Hill). The Gawler Craton in South Australia and Yilgarn Craton in Western Australia also have significant paleovalley-hosted uranium resources. In these regions, uranium-rich Proterozoic crystalline basement provides widely distributed potential source rocks (e.g., Hiltaba Suite granites) (Hou et al., 2007b). Felsic rocks at the margins of Amadeus and Ngalia basins in Northern Territory contain up to 32 ppm and 55 ppm uranium respectively (OZCHEM database). The felsic rocks also host uranium-bearing pegmatite bodies and fluorapatite veins, which are additional sources of leachable uranium (Jaireth et al., 2015). Schmid et al. (2012) identified hydrothermally-altered granite as the primary source of uranium and vanadium in the Bigrlyi sandstone-hosted deposits (Ngalia Basin) with the distribution of detrital vanadium mica (roscoelite) an important factor in the localization of secondary uranium and vanadium mineralization.

All known calcrete-hosted uranium deposits/prospects are located in paleovalleys that are incised across potential source rocks containing potassium, uranium and vanadium. Intensive weathering and erosion of these rocks provides uranium, vanadium, and potassium to the calcrete-hosted uranium system. Mafic igneous rocks, sediments with vanadium-rich clays, and ironstones (e.g., banded iron-formation and ferricrete) are the most likely sources of vanadium (Bastrakov et al., 2010). Felsic rocks in the vicinity of calcrete-hosted uranium deposits/prospects in the Yilgarn Craton contain up to 20 ppm uranium (Schofield, 2009). In the headwaters of drainage for the Lake Way deposit outcropping monzogranite (adamellite) at Mount Cleaver with altered monazite, ilmenite and zircon (with metamict alteration halos) contains up to 12 ppm uranium and up to 50 ppm vanadium and is a probable source for the Lake Way surficial uranium deposit (French and Allen, 1984), along with granite containing up to 25 ppm uranium (Mann and Deutscher, 1978). Uranium concentrations (up to 400 ppb) are recorded in ground waters in the Lake Way area (Mann and Deutscher, 1978).

In northern China, pre-Jurassic rocks, particularly the Archean and Paleoproterozoic basement, contain relatively high concentration of uranium; these represent a significant uranium source for Mesozoic paleovalley-related uranium deposits (Li et al., 2008). The source rocks of the northeastern Ordos Basin sediments, for instance, are high in uranium; strata of middle Variscan – early Yanshan ages typically contain an average of 4 ppm U and Indosinian granites contain 12 ppm U (Li et al., 2007a). These have contributed significant quantities of uranium for paleovalley-hosted

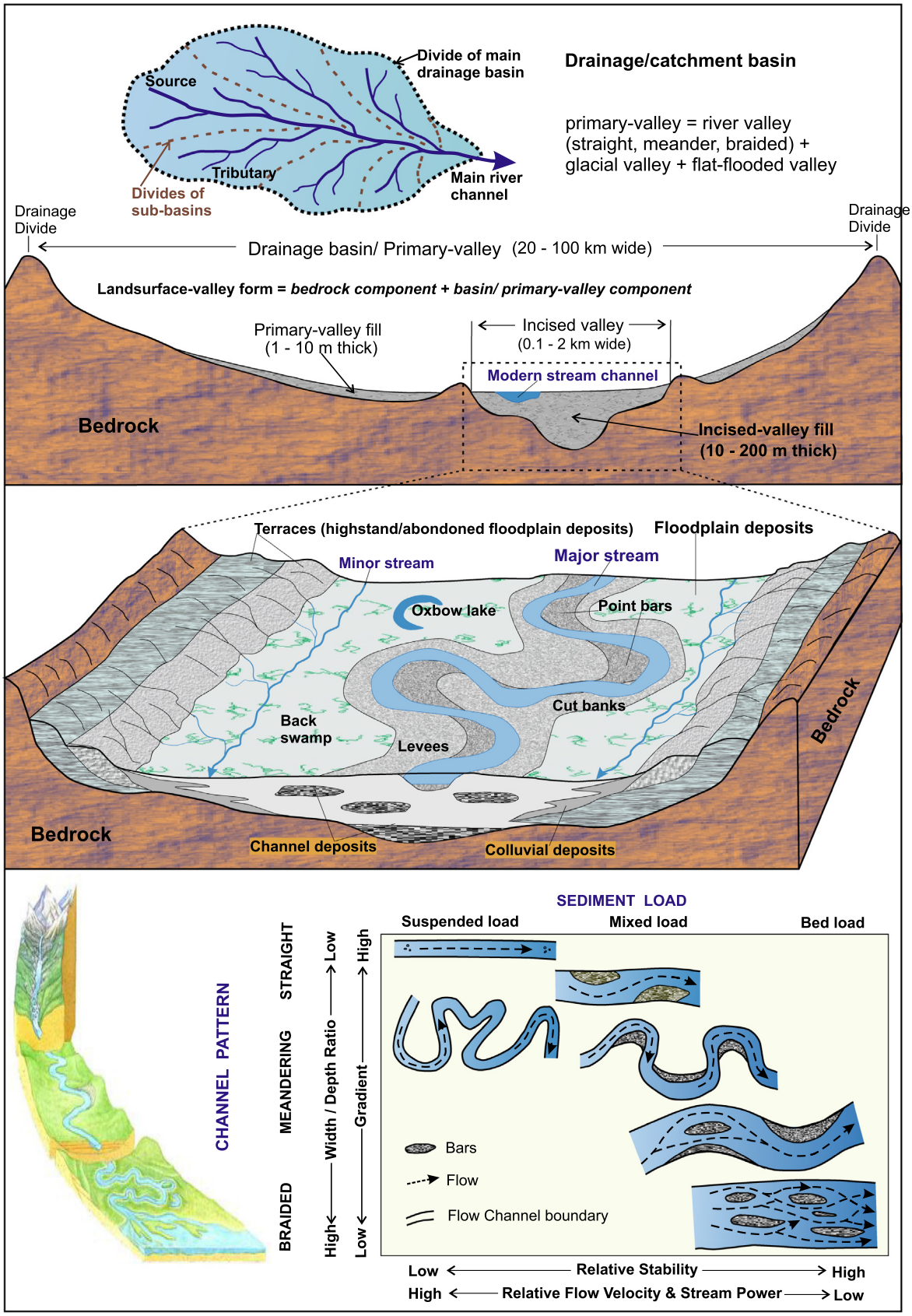

Fig. 3. Major geomorphic and stratigraphic components of typical paleovalleys developed in Australia and north China (after Schumm, 1981; Hou et al., 2001a; de Brockert, 2002).

Table 2
Major paleovalley-related uranium deposits and prospects of Australia and China (modified after). information sourced from Mckay and Miezitis, 2001; Roach et al., 2014; Wilson, 2015; Jaireth et al., 2015; CNNC and Geoscience Australia's OZMIN database).

Name	Field	Host unit & age	Main type	Ore (Mt)	Grade (%)
Angela	Amadeus Basin, NT	Undandita Member, Late Devonian to Late Carboniferous	Roll front	10.7	0.111
Bayinwula	Erlian Basin, N China	Saihan Formation, Cretaceous	Roll front, Basal channel	–	0.01–0.03
Bennett Well	Carnarvon Basin, WA	Birdrong Sandstone and Yarraloola Conglomerate, Cretaceous	Basal channel	26.7	0.023
Beverley	Callabonna Sub-basin, SA	Namba Formation, Neogene	Basal channel, Tabular	12.0	0.153
Big Lake	North of Lake Frome, Eyre Basin, SA	Namba Formation, Neogene	Basal channel, Tabular	–	0.024
Bigrlyi	Ngalia Basin, NT	Mount Eclipse Sandstone, Late Devonian to Late Carboniferous	Roll front	7.5	0.109
Billeroo	Billeroo Paleovalley, Callabonna Sub-basin, SA	Eyre Formation, Paleogene	Basal channel	12.0	0.025
Blackbush	Pirie Basin, SA	Kanaka Beds, Paleogene	Roll front, Basal channel	45.5	0.028
Carley Bore	Carnarvon Basin, WA	Birdrong Sandstone and Yarraloola Conglomerate, Cretaceous	Basal channel	13.8	0.033
Dongsheng	Ordos Basin, NW China	Zhiluo Formation, middle Triassic	Roll front, Tabular, lignite	–	0.03–0.05
Ealbara	Kingoonya Paleovalley, Eucla Basin, SA	Pidinga Formation, Paleogene	Tabular	–	–
Kalkaroo	Callabonna Sub-basin, SA	Eyre Formation, Paleogene	Basal channel	1.2	0.063
Four Mile East	Callabonna Sub-basin, SA	Eyre Formation, Paleogene	Roll front	4.1	0.310
Four Mile West	Callabonna Sub-basin, SA	Bulldog Shale, Cretaceous	Roll front	5.7	0.340
Goulds Dam	Callabonna Sub-basin, SA	Eyre Formation, Paleogene	Tabular, Basal channel	17.6	0.045
Honeymoon	Callabonna Sub-basin, SA	Eyre Formation, Paleogene	Tabular, Roll front	1.2	0.204
Kalkaroo	Callabonna Sub-basin, SA	Eyre Formation, Paleogene	Basal channel	910 t of U_3O_8	0.074
Junction Dam	Callabonna Sub-basin, SA	Eyre Formation, Paleogene	Basal channel	4.36	0.034
Manyingee	Carnarvon Basin, WA	Birdrong Sandstone and Yarraloola Conglomerate, Cretaceous	Basal channel	13.8	0.072
MacDonnell Creek	Callabonna Sub-basin, SA	Eyre Formation, Paleogene	Basal channel	–	0.250
Mulga Rock	Eucla/Narnoo Basin, WA	Narnoo Sequence, Paleogene	Tabular, Roll front, Basal channel, lignite	57.3	0.042
Narlaby	Narlaby Paleovalley, Eucla Basin, SA	Pidinga Formation, Paleogene	Tabular	–	0.005
Nuheting	Erlian Basin, N China	Erlian Formation, Cretaceous	Tabular, lignite	>10,000 t U	0.03–0.10
Oban	Lake Charles Paleovalley, Callabonna Sub-basin, SA	Eyre Formation, Paleogene	Tabular, Basal channel	8.2	0.022
Oobagooma	Canning Basin (Yampi Embayment), WA	Yampi Sandstone, Early Carboniferous	Roll front	8.2	0.102
Pannikin	Callabonna Sub-basin, SA	Eyre Formation, Paleogene	Roll front	–	–
Pepegoona	Callabonna Sub-basin, SA	Eyre Formation, Paleogene	Roll front	2.2	0.153
Pundinya	Wynbring Paleovalley, Eucla Basin, SA	Pidinga Formation, Paleogene	Tabular	–	0.041
Qian Jia Dian	Songliao Basin, NE China	Yaojia Formation Cretaceous	Tabular	–	–
Shashagetai	Ordos Basin, NW China	Zhiluo Formation, middle Triassic	Roll front, lignite	–	–
Shihongtan	Tuha Basin, NW China	Shuixigou Group, Jurassic	Roll front, Tabular	–	–
Walbiri	Ngalia Basin, NT	Mount Eclipse Sandstone, Paleozoic	Roll front	0.42	0.137
Warrior	Warrior Paleovalley, Eucla Basin, SA	Pidinga Formation, Paleogene	Basal channel	11.8	0.034
Wuyier	Yili Basin, NW China	Shuixigou Group, Jurassic	Roll front, Tabular	–	–
Wuyiyi	Yili Basin, NW China	Shuixigou Group, Jurassic	Roll front, Tabular	–	–
Wuyisan	Yili Basin, NW China	Shuixigou Group, Jurassic	Roll front, Tabular	–	–
Watson	Watson Paleovalley, Eucla Basin, SA	Pidinga Formation, Paleogene	Basal channel	–	0.010
Yagdin	Callabonna Sub-basin, SA	Namba Formation, Neogene	Basal channel	–	0.047
Yaninee	Yaninee Paleovalley, Eucla Basin, SA	Pidinga Formation, Paleogene	Basal channel / Roll front	–	0.145
Yarramba	Yarramba Paleovalley, Callabonna Sub-basin, SA	Eyre Formation, Paleogene	Basal channel/Roll front	–	–
Yarranna	Narlaby Paleovalley, Eucla Basin, SA	Pidinga Formation, Paleogene	Basal channel/Roll front	–	0.241

uranium deposits in the Ordos Basin (Li et al., 2008). The Indosinian magmatism (236.8 ± 5.8 Ma) in the Erlian Basin, which forms the basement to the eastern part of the Central Asia Orogenic Belt, is widely represented by U-Th-rich high-K calcalkaline granites derived from an enriched mantle This provides a major source of primary uranium that played an important role (see below) in the formation of the uranium deposits in Erlian Basin (Bonnetti et al., 2014).

2.2. Geological setting

The term 'paleovalley-related' implies more than just uranium hosted within sediments confined to the paleovalley proper and includes associated alluvial fans, fluvial/estuarine channels, deltas, and any intermittent fans/channels/deltas formed within sedimentary basin during the lowstands of a sedimentary basin development (Fig. 3). The various styles of uranium mineralization associated with these systems can include any sedimen tary/diagenetic/epigenetic concentration of uranium minerals occurring in fluvial, alluvial, lacustrine, and estuarine sediments. As fluvial paleosystems are developed within ancient topographic features that define host paleovalleys, recognition of these features in the present-day landscape is important in establishing physical links to primary uranium source rocks and in determining the pattern of groundwater flow at the time of uranium deposition.

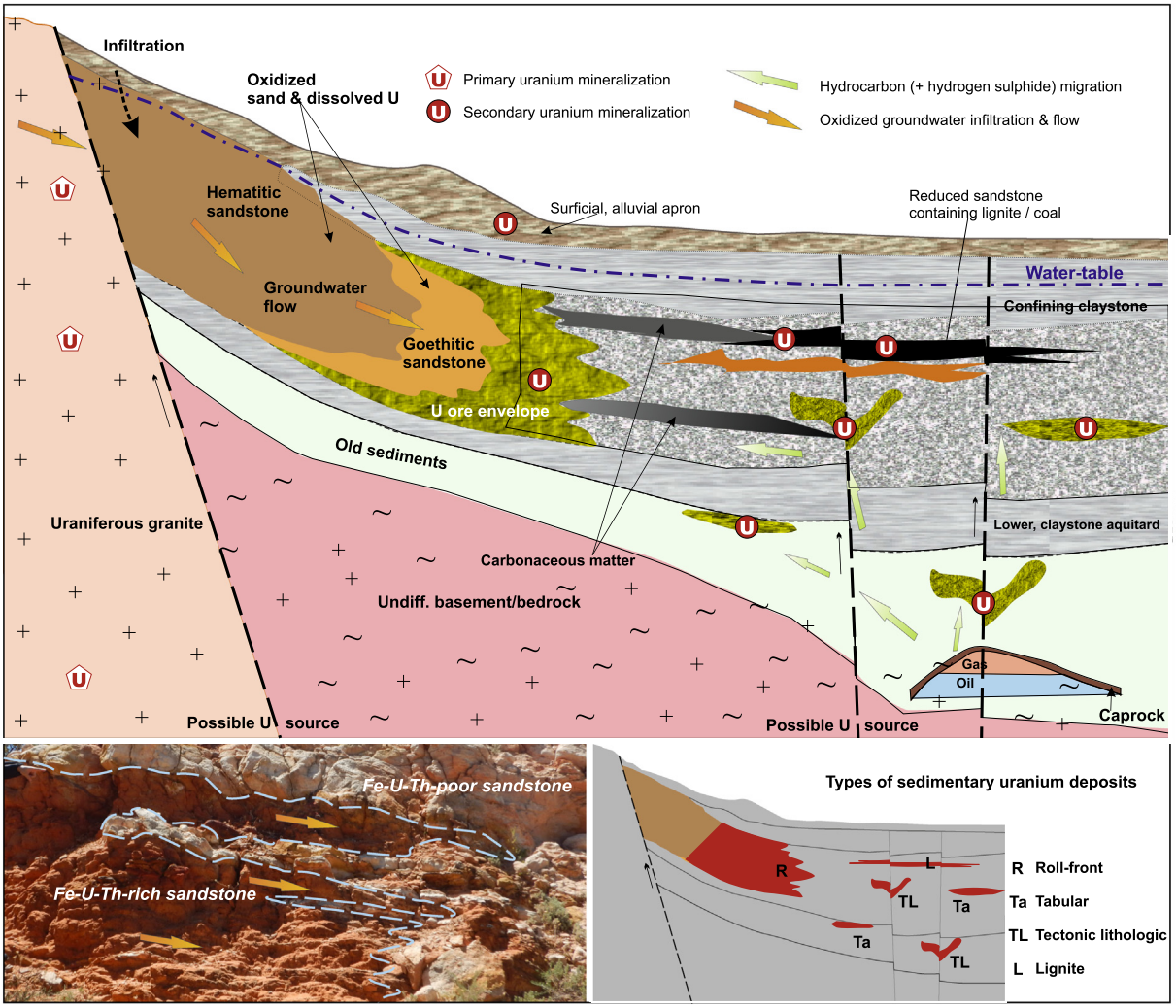

Fig. 4. Palinspastic cross-section model for sedimentary uranium deposits, highlighting the role of aquifer flow (e.g., Devoto, 1978a) and REDOX state, formation of roll-front mineralization and the stratigraphic relationship of basal channel, tabular, tectonic lithological and lignite uranium mineralization. Idealized from examples of South Australia. The photo shows multiple paleoredox fronts in the middle Eyre Formation (see Fig. 7), Dead Tree section at Foul Mile West deposit of South Australia (Fig. 1B) (after Hore and Hill, 2009).

In channel deposits, the distribution of uranium mineralization is generally influenced by the shape of the paleovalley and associated fluvial channels. Uranium mineralization is distributed variously in basal scours (e.g., Blackbush deposit in South Australia), bends (e.g. the Honeymoon and East Kalkaroo deposits, South Australia), sites of confluences with tributaries (e.g., Beverley, Goulds Dam and Oban deposits, South Australia), and areas of channel-widening and bar-heads (e.g., Dongsheng and Qianjiadian deposits, China) (Cai et al., 2005, 2007a; Li et al., 2008; Hou et al., 2014; Jaireth et al., 2015). Many paleovalley-related uranium deposits, particularly the sandstone-hosted uranium mineralization, are structurally controlled, in which the deposits appear to result from uranium-bearing oxidized waters mixing with mobile reductants channeled along permeable structures (e.g., Sun et al., 2009; Goldhaber et al., 1983; Michaelsen et al., 2016). The mineralization in the tectonic-lithologic type of sandstone-hosted uranium deposits (e.g., uranium deposits in the Chu-Sarysu basin in Kazakhstan, the uranium deposits in the Lake Frome region, South Australia and the Mikouloungou deposit in the Franceville Basin, Gabon) is controlled by permeable fault zones with mineralization extending into clastic sediments adjacent to the fault (Fig. 4) (Aubakirov, 1998; Hou et al., 2014; Jaireth et al., 2015). In districts with uranium deposits underlain by hydrocarbon basins, tectonically active structures often are effective conduits for mobile reductants (i.e. hydrocarbons) and thereby provide an important control on the distribution of uranium deposits (Jaireth et al., 2008; Li et al., 2008; Michaelsen et al., 2016). For example, in the Dongsheng area of the Ordos Basin, China, evidence of upward seepage of petroleum along fault F1 (Zhang et al., 2006) is identified by Cai et al. (2007a) as the source of abundant organic carbon for uranium biomineralization by bacteria to form sandstone-hosted uranium deposits in the shallower basin sediments.

2.3. Mineralization and preservation

The uranium is leached under oxidizing and slightly acidic conditions and is mobilized in alluvial/fluvial systems and in groundwater moving through the sediments, with precipitation of uranium commonly through interaction with reductants to form uranium ore bodies as part of the processes of diagenesis and epigenesis of the host sediments (Fig. 5) (e.g., Dahlkamp, 1993). The age of sandstone/lignite-hosted uranium mineralization is typically younger than that of the host sediment and commonly formed during more than one episode (e.g., Erlian Basin, see

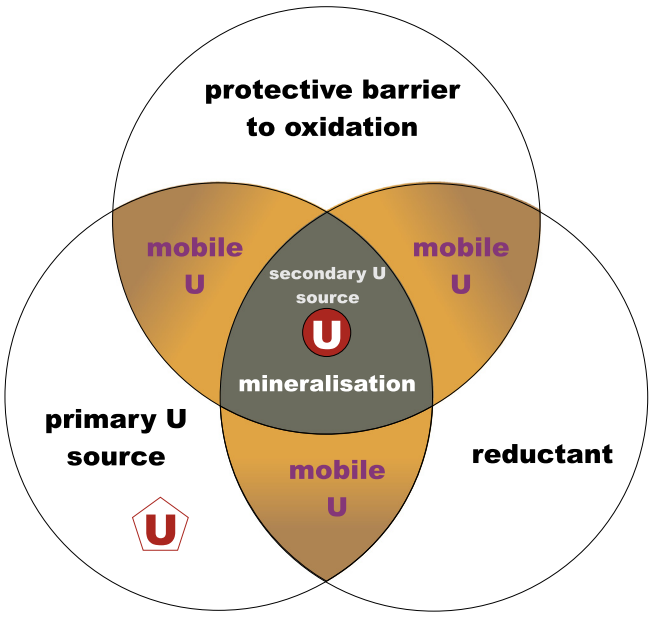

Fig. 5. Schematic illustration of the junction of three independent parameters required to form sandstone uranium deposits (from Hou et al., 2014).

below), particularly in the interlayer oxidation mineralization system (e.g., Ordos Basin; Cai et al., 2007a; Li et al., 2007a). In the Callabonna Sub-basin, for instance, the age of coffinite grains (6.7 Ma–0.4 Ma) at the Beverley deposit and carnotite (5.5 Ma–3.4 Ma) disseminated in the Beverley Sands (upper mineralization zone) suggest that uranium mineralization (coffinite and carnotite) commenced during Pliocene time (6.7 Ma–3.4 Ma), soon after the sediments were deposited and the mineralization continued to be modified for at least 3 Ma (Wülser et al., 2011). In the Yili Basin uranium mineralization is of Pliocene age (5–2 Ma) but hosted in Jurassic (~178 Ma) sediment (see below).

In paleovalley-related uranium systems, oxidation-reduction reactions predominantly control the transport (in oxidized conditions) and deposition (in reduced conditions) of the uranium that is particularly concentrated along redox-front zones. Worldwide, paleovalley-related uranium deposits formed predominantly during the youngest stage of the five atmosphere oxygenation stages (540 Ma to present), while the atmospheric oxygen levels probably rose to a maximum value of ~0.3 atm (Holland, 2006). In relation to reduction, the vascular plants on the Earth, and the consequent accumulation of terrestrial hydrocarbon, have largely developed since the Late Silurian (Cuney, 2010). Consequently, paleovalley-related uranium deposits were formed mostly post-Silurian, and particularly during the Mesozoic and Cenozoic eras (Fig. 6; Hou et al., 2014), when rising levels of atmospheric oxygen enhanced intraformational redox gradients and provided ideal conditions for the formation of these terrestrial uranium deposits (Jaireth et al., 2015).

Preservation is a significant factor for paleovalley-related uranium deposits, because fine-grained uranium mineralization, mostly in weakly consolidated sediments, can be partially or completely dispersed, particularly in the deposits formed at shallow depths, by post-mineralization erosion and uplift, and/or can be remobilized and degraded by oxidized waters flowing through

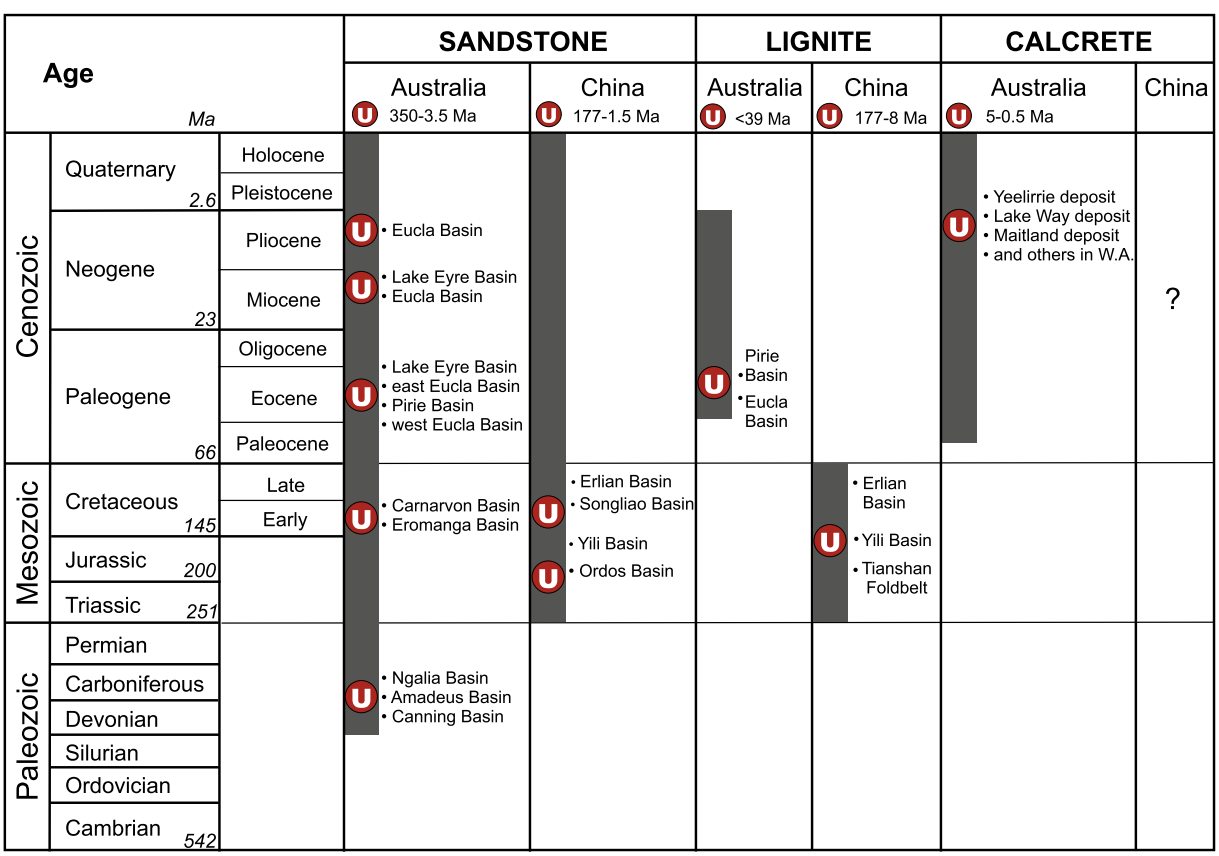

Fig. 6. Distribution of sandstone, lignite and calcrete-hosted uranium deposits in Australia and China through geological time (for the deposits located in the basins/regions see Fig. 1), and age-ranges (grey vertical bars) of the three types of paleovalley-related deposits worldwide. Note: for these three deposit types the ages shown are those of the host rocks (modified from Hou et al., 2014).

the aquifer host-rocks. This is the case for uranium deposits, such as Jackpile-Paguate deposit, northwest New Mexico (Adams et al., 1978), Pepegoona deposit, South Australia (Murphy et al., 2011), and uranium mineralization of Chu-Sarysu Basin in Kazakhstan (Fyodorov, 2001a,b).

In calcrete-uranium systems, uranium and vanadium are transported in oxidized groundwaters and carnotite is deposited, as a result of groundwater mixing or changes in pH, and the concentration of CO_2 caused by seasonal fluctuation of groundwater levels. The fluctuation is associated with evaporation of groundwaters, which can lead to an increase in the concentration of dissolved potassium, vanadium and uranium (Butt et al., 1984). The relatively young age and continuous dissolution and precipitation caused by the influx of waters in the channel aquifers resulted in uranium disequilibrium in calcrete-hosted deposits (Dickson, 1984). Therefore the age of mineralization for this type deposits is estimated typically by examining the uranium series disequilibrium and geological setting, such as the calcrete-hosted deposits in the Yeelirrie deposits (0.1 Ma–0.7 Ma) in the Yilgarn Craton, WA (Dickson, 1984), and Langer-Heinrich deposits (>0.5 Ma) in Namibia (Kyser and Cuney, 2009). The preservation of calcrete-hosted uranium mineralization is a critical factor as the deposits form in relatively young paleovalleys that continue as present day aquifers. The existence of such deposits is due either to preservation of mineralization or to continuous enrichment of mineralization by addition of uranium and vanadium mobilized from sources upstream. The deposits are readily degraded (partially or completely) by altered environmental conditions that may result from tectonic activity, landscape modification, or climate change (e.g., Boyle, 1984).

2.4. Sandstone-hosted uranium deposits

Sandstone uranium deposits contain diagenetic and/or epigenetic concentrations of uranium minerals, usually uraninite or coffinite and are typically hosted by fine to coarse-grained sand deposited in fluvial, alluvial, lacustrine or marginal marine environments. The majority of deposits (e.g., in USA, Kazakhstan, Australia, China, Niger, Uzbekistan, Gabon, and South Africa) occur in essentially undisturbed continental sandstones of Mesozoic and Cenozoic (mostly Paleogene and Neogene) ages (Finch and Davis, 1985; McKay and Miezitis, 2001). Deposits in older host rocks are known, but are less common (e.g., Paleozoic sandstone-hosted uranium roll-fronts in Western Australia and Europe (IAEA, 2009). In Australia, the uranium districts and basins containing sandstone-hosted uranium deposits are the Lake Eyre Basin, Eucla Basin, Westmoreland, Pandanus Creek district, Amadeus Basin, Ngalia Basin, Gunbarrel Basin, Carnarvon Basin and Canning Basin (Fig. 1). The significant sandstone uranium deposits in China are located mostly in northern China, including the Yili, Ordos, Erlian and Songliao basins (Fig. 2). Recently, other areas with potential to host economic uranium resources have been identified through greenfield discoveries, including the Pirie Sub-basin in South Australia (e.g., Blackbush deposit) and Cenozoic paleovalleys in the south-east of Western Australia (e.g., Theseus deposit).

Within many sandstone deposits, low permeability shale/mudstone (sometimes lignite or coal) units are typically interbedded in the sedimentary sequence and may occur immediately above and below the mineralized sandstone. The presence of redox fronts within many uranium deposits is consistent with uranium deposition by reduction of oxidized U-bearing fluids flowing in sandy aquifers. Uranium, as U^{6+} is readily reduced to $U^{4+}$to form insoluble precipitates (e.g., Bastrakov et al., 2010). Reducing agents encountered within the sandstone include: carbonaceous material (e.g., detrital plant debris and marine algae), sulfides (pyrite, H_2S), petroleum (including gas), and Fe^{2+} released during mineral alteration (e.g., interbedded mafic volcanics with abundant ferro-magnesian minerals, such as chlorite). Mobile reductants may be generated from external sources such as hydrocarbon-bearing sediments from deeper regions of a basin beneath or flanking sandstone-hosted uranium deposits, or from proximal sources such as biogenic and non-biogenic H_2S produced from the interaction of groundwater with pyrite in the sandstone (Spirakis, 1996). The role of H_2S as an effective reductant was demonstrated by Goldhaber et al. (1978) and Reynolds and Goldhaber (1978) in South Texas for roll-type uranium deposits hosted by organic-poor sandstone. In recent years, many authors (e.g., Huang et al., 2005; Min et al., 2005a,b; Cai et al., 2007a,b; Li et al., 2008; Jaireth et al., 2008, 2015; Pechenkin, 2014; Bonnetti et al., 2014, 2015a,b) have reported on the role of mobile reductants (hydrocarbons and associated gases, such as H2S, CH4, N2 and H2) in the formation of various sandstone-hosted uranium deposits.

A general model of sandstone-hosted uranium deposits widely used to guide exploration is that uranium is liberated from a source rock area and is mobilized and circulated in oxidized fluids/groundwaters through porous strata until it encounters a reducing environment where it is precipitated; i.e., uranium mineralization results from the interaction of uranium-rich oxidizing fluids and reduced lithologies or mobile reductant (at redox fronts) (Fig. 4) (e.g., Adams and Smith, 1981; Dahlkamp, 1993; De-Voto, 1978a; Fischer,1970; Goldhaber et al., 1983; Grutt, 1971; Nash et al., 1981). The uranium source, aquifer dynamics, and type and abundance of reductant in the ore-bearing sedimentary sequence are key factors in the formation of sandstone uranium deposits. Sediments in close proximity to the redox boundary typically show yellow to orange coloration resulting from iron oxyhydroxide precipitates on the oxidized side of the redox boundary, changing progressively towards darker tones within reduced sediments. The locations of uranium ore deposits reflect the interplay of uranium source, sedimentary facies, uranium-bearing fluids/groundwater, and the concentration and distribution of reducing agents (viz. carbonaceous matter, sulfides, hydrocarbons, or Fe^{2+} ions from various sources including interbedded ferro-magnesian-rich mafic volcanic; e.g., Spirakis, 1996).

Based on the shape of the orebody and its relationship to the depositional or structural environment, sandstone uranium deposits can be subdivided into four types (including significance in terms of relative percentage of known resources) (IAEA, 2009): roll-front (54%), tabular (37%), basal channel (7%) and tectonic-lithologic (2%) (Fig. 4; these may be gradational into each) (e.g., Fischer, 1970; De-Voto, 1978b; Nash et al., 1981; Dahlkamp, 1993). Roll-front deposits form arcuate bodies of mineralization that cross-cut sandstone bedding. Tabular deposits commonly occur as irregular, elongate and lenticular bodies parallel to the depositional trend in paleovalleys. Basal channel deposits include uranium mineralization distributed in paleovalleys that incise underlying uranium-bearing crystalline basement or sedimentary bedrock (e.g., Honeymoon and Blackbush in South Australia and examples from China, Canada and Russia) (Boyle, 1982; Bush, 2000; IAEA, 2009; Li et al., 2008). Tectonic-lithologic deposits occur in sandstones adjacent to permeable fault zones; (e.g., Dongsheng deposits, northern China) (Li et al., 2008). The hydraulic head potential gradient largely controls continuous flux of groundwater that may be enhanced by during periodic uplift of the basement rocks forming the basin margins (Dahlkamp, 1993; Sanford, 1994). These deposits are characterized by strong structural control of mineralization, which is distributed along high-angle tectonic faults cutting the host sedimentary sequences (Dahlkamp, 1993; IAEA, 2009). Tabular, basal channel and roll-front mineralized bodies generally form along the contact between sand and clay horizons and at the base or margins of paleochannel, while tectonic/lithologic deposits are distributed along fault zones and

in adjacent permeable sandstone units. The idealized structure of uranium mineralization concentrated along a distinct boundary at or near the contact with reduced sedimentary environments, as shown in Fig. 4, may not always be obvious, due in part to later diagenetic and epigenetic modifications of the orebody. Evidence of environmental factors controlling uranium deposition can be obscured, or completely destroyed, by multiple groundwater and/or hydrothermal pulses, in particular, when uranium mineralization is modified and partly remobilized by post-ore, reduced/oxidized and saline fluids (Abzalov, 2012).

Many of Australia's sandstone-hosted uranium deposits occur in paleovalleys and related terraces developed within and peripheral to sedimentary basins of Carboniferous, Cretaceous and Cenozoic age (Figs. 1, 3 and 6). Around 46% of sandstone-hosted uranium resources are contained within the Cenozoic Callabonna Sub-basin (southern Lake Eyre Basin) in South Australia. Other deposits are located in Western Australia and Northern Territory (Table 2) (Jaireth et al., 2015). In China, Mesozoic sedimentary basins, including the Ordos, Songliao, Erlian and Yili basins of north China contain significant paleovalley sandstone-hosted uranium deposits (see below). The Songliao Basin and Ordos Basin, in particular, are also significant source areas for oil, gas, and coal production.

2.4.1. Carnarvon, Canning, Amadeus and Ngalia basins, Australia

The geology of some major deposits and prospects located in these basins are described in Curtis et al. (1990), McKay and Miezitis (2001) and Lally and Bajwah (2006). Several roll-front sandstone-hosted uranium deposits in Western Australia, including Manyingee and Carley Bore, occur along the eastern margin of the Carnarvon Basin (Fig. 1), preserved in a paleovalley of Cretaceous age between basement highs (Penney, 2012). Theseus deposit, discovered in 2009 in Western Australia close to the border of the Northern Territory, comprises roll-front uranium mineralization hosted within an Eocene paleovalley that drained the region between the Ngalia Basin and crystalline basement of the Arunta Province (Penney, 2012). Afghan Swan prospect in the Northern Territory, is hosted in early Cenozoic sands deposited near the base of paleovalleys developed in the central area of the Ngalia Basin and is another recent (2010) discovery of paleovalley-related uranium (Thundelarra Exploration Ltd, 2012). Bigrlyl and Walbiri deposits occur along the northern margin of

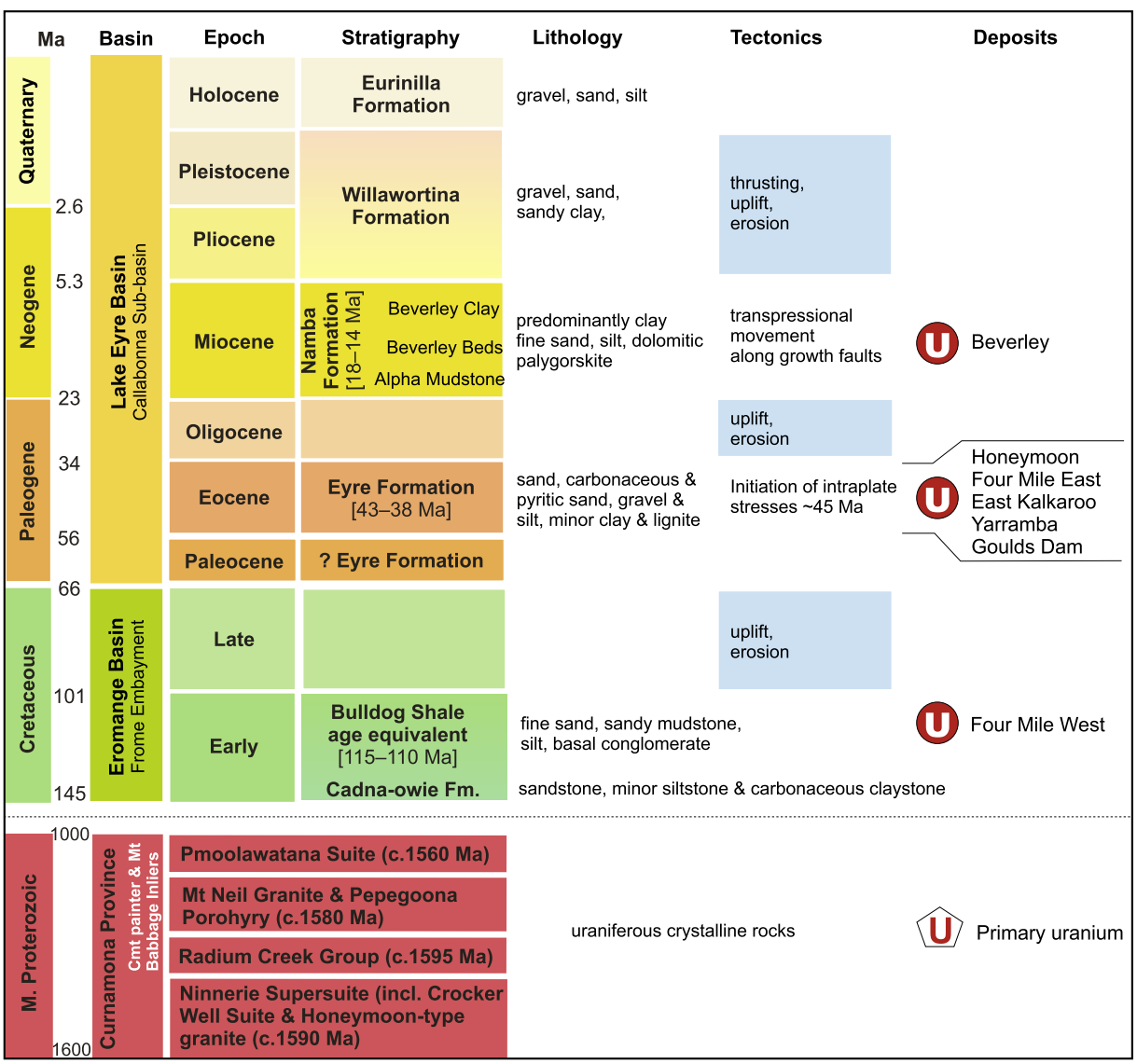

Fig. 7. Stratigraphic position of the sandstone uranium deposits and primary uranium source/mineralization in the Lake Frome region, South Australia.

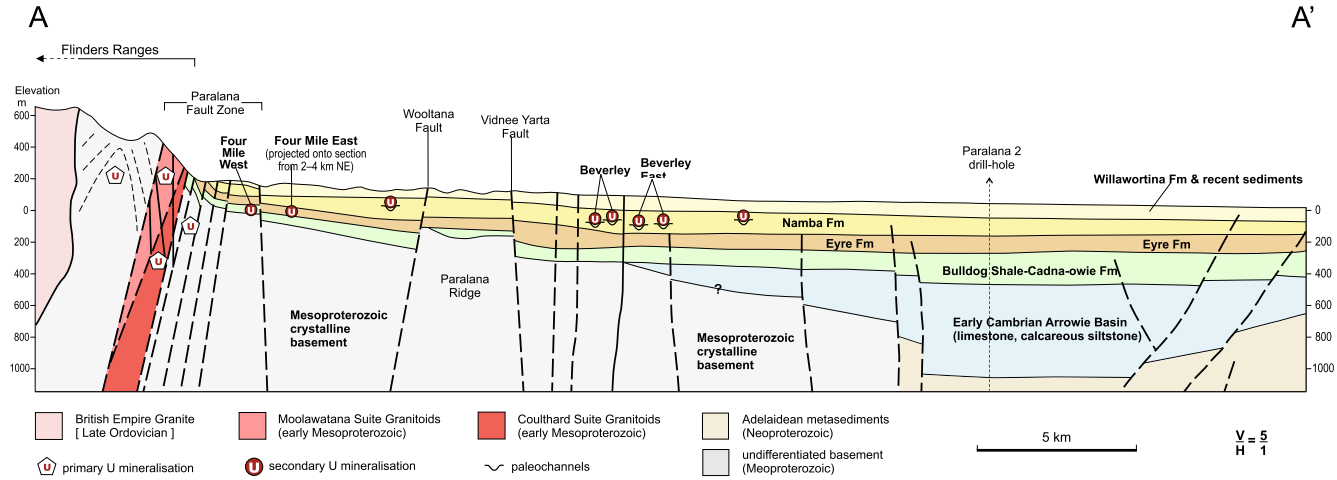

Fig. 8. Idealized geological cross-section across the Lake Frome region (after Hou et al., 2014, 2012; Michaelsen et al., 2016). For the location of the cross-section see Fig. 1B.

the Ngalia Basin where the host rocks were deposited in a braided-fluvial system of late Devonian-Carboniferous age (Fig. 6; e.g., Fidler et al., 1990). To the south, Angela and Pamela deposits, in the Amadeus Basin, were formed in a similar stratigraphic setting to deposits in the Ngalia Basin (Borshoff and Faris, 1990). In the Canning Basin, in northern Western Australia, the Oobagooma uranium deposit is hosted by the Yampi Sandstone (Early Carboniferous) within a fault-bound paleodrainage system, with high-grade uranium mineralized zones formed in classic roll-fronts in sediments with abundant organic matter and pyrite (McKay and Miezitis, 2001; Brunt, 1990).

Deformation and exhumation is also significant for the sandstone-hosted uranium deposits in the Amadeus (Angela and Pamela deposits) and Ngalia basins (Bigryli and Walbiri deposits) (Fidler et al., 1990; Borshoff and Faris, 1990). The deformation during the 450 Ma–300 Ma Alice Springs Orogeny resulted in exhumation of the basement, which became a major source of detritus for the host rocks, the Brewer Conglomerate (Amadeus Basin) (Edgoose, 2013a) and the Late Devonian to Carboniferous Mount Eclipse Sandstone (Ngalia Basin) (Edgoose, 2013b). The source rocks of both these units included uranium-rich granites of the Arunta Region (Jaireth et al., 2015). The subsequent peak of deformation terminated deposition in the basins and initiated major thrusting and associated thrust-related folding within and adjacent to the basins (Edgoose, 2013a, b).

2.4.2. Callabonna Sub-basin of the Lake Eyre Basin, South Australia

Callabonna Sub-basin is Australia's premier sandstone-hosted uranium province, located in the southeastern part of the extensive Lake Eyre Basin (Cenozoic) that comprises thick (in places > 400 m) episodic fluvial, alluvial and lacustrine sediments (Callen et al., 1995). The Callabonna Sub-basin overlies the Frome Embayment portion of the Eromanga Basin (Mesozoic) and sedimentary rocks of the Adelaide Geosyncline (Neoproterozoic) and Arrowie Basin (Cambrian) but mostly extends across weathered crystalline basement of the Paleo-Mesoproterozoic Curnamona Province. The north-western margin of the Callabonna Sub-basin is adjacent to the U-rich Mesoproterozoic basement of the Mount Painter inlier that is uplifted 100 to 200 m above the basin as the result of episodic neotectonic activity commencing in the early Cenozoic (Fig. 1B). Uranium-enriched rocks of the northern Flinders Ranges and Olary region, including numerous small uranium vein and breccia-hosted deposits within crystalline rocks, such as the Mount Painter Inlier, provide an abundant source of uranium for ongoing dispersion into the Callabonna Sub-basin (Fig. 7).

The lower U-bearing unit of the Callabonna Sub-basin (southern part of the Lake Eyre Basin) is the Eyre Formation that is comprised of fluvial sandstone, lignite, carbonaceous clastics and mudstone (Fig. 7). Overlying the Eyre Formation, clays, sands and carbonates of the Namba Formation were deposited in extensive lakes and associated fluvial and shoreline environments, which were blanketed subsequently by Pliocene to Quaternary colluvial, fluvial, aeolian and playa-lake sediments, in response to drier climatic conditions across the interior of the Australian continent. The upper uranium host unit (e.g., Beverley mineralization) is Namba Formation (Miocene) in Neogene sandy paleochannel incised across a thick mudstone sequence. Regionally, the Namba Formation is mainly clay and silt, intercalated with minor fine-grained channel sand with subordinate carbonate and sapropelic coal near the base (Michaelsen et al., 2016). To the west of the Birdsville Track Ridge, the Tirari Sub-basin (northern part the Lake Eyre Basin) also has potential to host sedimentary uranium within paleovalleys (Fig. 1B; Hou et al., 2006).

Several major faults are considered to have played important roles in determining the present-day and paleo-architecture of the northern Callabonna Sub-basin, including the Paralana Fault Zone, Vidnee Yarta Fault and Wooltana Fault (Heathgate Resources, 2007). Drillhole and geophysical data suggest that the block defined by the Wooltana Fault and Vidnee Yarta Fault forms an upthrusted inlier (the Paralana Ridge) separating the Beverley deposit to the east from the Four Mile deposits in the Paralana Embayment (Fig. 8) (Heathgate Resources, 2008). Movement on the Poontana Fault Zone could also have controlled the alignment of the Miocene paleovalley which hosts the Beverley deposit (Heathgate Resources, 2007).

Uranium deposits including Beverley, Four Mile East, Four Mile West, Pepegoona and Pannikin occur in the northern Callabonna Sub-basin (Fig. 1B; Table 2). Four Mile East deposit, Pannikin and Pepegoona deposits are predominantly hosted within alluvial fans and amalgamated fluvial sands of Eocene age (Eyre Formation), whereas Beverley deposits occur in the Miocene fluvial sediments of Namba Formation (Heathgate Resources, 1998). Four Mile West deposit is hosted within sandy sediments of the Mesozoic Frome Embayment of the Eromanga Basin (Cross et al., 2010) beneath sediments of the Callabonna Sub-basin (Stoian, 2010). Mineralization at Four Mile West is dominantly uraninite, along with various REE and U-bearing phosphate minerals and associated pyrite and kaolinite. The host sandy and diamictite facies of the Bulldog Shale (late Early Cretaceous; Fig. 7) (Stoian, 2010) were deposited during marine onlap of the crystalline basement of the Mount Painter

Inlier (Fig. 8) (e.g., Michaelsen et al. 2012). The diamictite reflects conditions of Early Cretaceous glaciation previously recognized in the region from lodgement till deposits in the overlying Cadnaowie Formation (Alley and Frakes, 2003). The Four Mile deposits are on the margin of the Frome Embayment and proximal to primary uranium mineralization in crystalline basement rocks of the Mount Painter Inlier (Figs. 1 and 8). The ore zones are situated between the Paralana Fault Zone, which defines the eastern edge of the northern Flinders Ranges, and the Poontana and Wooltana faults, where basement has been uplifted in a horst structure forming a barrier to easterly groundwater flow within the Cretaceous and Eocene sediments (Fig. 8). The combined indicated and inferred resource at Four Mile West and Four Mile East deposits is 9.8 million tonnes at 0.33% U_3O_8, containing 32 000 tonnes U_3O_8 which make this the largest and highest grade sandstone-hosted uranium district in Australia (Penney, 2012; Johnstone, 2013). In the Pepegoona Deposit, uranium-bearing sands of the Eyre Formation are within 200 m of outcropping Mesoproterozoic granites of the Mount Painter Inlier. The mineralization is developed within complex redox fronts. The ore zone is overlain by a thin groundwater silcrete, and this in turn, is overlain by Namba Formation silts and Willawortina Formation gravels. The host sands are underlain by Cretaceous silts of the Bulldog Shale (Fig. 6) (McConachy, 2009). Further to the north, drill intersections record uranium in several sand horizons within the Namba Formation at Yagdlin prospect, approximately 12 km north of Beverley (Giralia Resources, 2007).

To the east of the Paralana Ridge, the mineralization (mainly coffinite coating quartz grains and infilling void space) of Beverley deposit, assuming tabular and lenticular bodies, is hosted by sandy infill of Namba Formation within a broadly north-south striking paleovalley system, immediately east of Poontana Fault zone. In the Namba Formation, the lenticular Beverley Sands (hosting Beverley Deposit) are interbedded between the Beverley Clay and the Alpha Mudstone that contains plant fragments and large pieces of carbonized wood (Fig. 7) (Heathgate Resources, 2007). Uranium mineralization is present also within the 'Alpha sequence' at the Beverley East satellite deposit (Marsland-Smith et al. 2011). The Beverley Sands aquifer is made up of four units, of which the main mineralized sands have moderate permeability, whereas the two underlying sandy units are more permeable (Heathgate Resources, 2007). Development of the Beverley paleochannel was controlled by *syn*-sedimentary activity on the Poontana Fault system (Fig. 8). In addition to coffinite, there is subordinate uraninite (as nodules) and very minor carnotite (Wülser et al., 2011). U-mineralized nodules nucleated around Co-rich pyrite with S isotope compositions ($\delta^{34}S = 1.0 \pm 0.3‰$) suggestive of early diagenetic lacustrine origin (Wülser et al., 2011). Michaelsen and Fabris (2014) identified six organic facies, of which three are in the Eyre Formation and two are in the Namba Formation (e.g., liptinite, lamalginite and telaginite). Michaelsen and Fabris (2011) considered that mobile reductants (hydrocarbon gases) could have been involved in the formation of the Beverley and other uranium deposits in the northern part of the Lake Frome region, as the upper Namba Formation lacks effective (hydrogen-rich detrital organic) reductants. The hydrocarbon gas derived from the maturation of organic matter within the Poontana Trough (Fig. 8) is suggested to be the most plausible uranium reductant that can be implicated in the formation of the Beverley uranium deposit (Michaelsen et al., 2016). U-Pb dating of coffinite and carnotite indicates that uranium mineralization formed predominantly during Pliocene time (6.7–3.4 Ma; Wülser et al., 2011), corresponding to an episode of uplift and erosion of the northern Flinders Ranges and deposition of alluvial fans comprising the Willawortina Formation, which overlies the Namba Formation.

Cenozoic paleovalleys, with headwaters in the eroded, weathered basement rocks of the Olary region, incised Cretaceous and older rocks across the southern half of the Callabonna Subbasin (Conor, 2004), and coalesced to form amalgamated blanket-sands towards the centre of the basin (Callen, 1990). Several uranium deposits have been delineated within the Paleogene paleovalley systems (Table 2; Figs. 1 and 7), which generally run northward from the uplifted parts of the Olary Domain (Alley, 1998; Hou et al., 2007a,b, 2012). These include Oban deposit in the Lake Charles paleovalley (Curnamona Energy, 2009; Tonkin, 2009), the East Kalkaroo deposit in the Yarramba paleovalley (Uranium One, 2007), the Goulds Dam deposit and the Billeroo prospect in the Billeroo paleochannel near the confluence with the Curnamona paleovalley (Curtis et al., 1990; Reif, 2000), the Yarramba prospect in the Yarramba paleovalley, and Junction Dam prospect (18 km east of Honeymoon deposit) (Wilson, 2015). Significant uranium anomalies have been reported from other paleovalleys, including the Curnamona paleovalley, Erudina paleovalley, Wyambana paleovalley, and Stickhole paleovalley (Fabris et al., 2004).

Honeymoon deposit is hosted by sub-horizontal permeable sands of the Eocene Eyre Formation (Table 2; Figs. 2 and 7). Here, Eyre Formation consists of immature, pyritic, carbonaceous sands and gravels interbedded with lignite and kaolinite-illite-montmor illonite clays. The sands are overlain by thick Miocene clays of the Namba Formation. The Yarramba paleovalley drained and incised weathered basement rocks of the southern Curnamona Province and was infilled by up to 50 m of (now uranium-bearing) Eyre Formation, occurring as three sand members, the 'basal sand', 'middle' and 'upper sands', which are separated by clay layers (Reif, 2000). Uranium mineralization, primarily as coffinite, occurs in five distinct horizons separated by thin clay seams and was sourced from nearby uraniferous granite (Honeymoon-type granites) (Fricke, 2008; Fricke and Reid, 2009). The Honeymoon deposit was formed at an extensive reduction-oxidation boundary at the paleovalley margins (Reif, 2000; Hou et al., 2007b).

2.4.3. Eucla Basin, Australia

The Eucla Basin and its peripheral paleovalleys, stretching from the eastern Yilgarn Craton of Western Australia to western Gawler Craton of South Australia (e.g., Benbow et al., 1995; Alley et al., 1999; Clarke, 1993; Hou et al., 2003; 2007a; 2011; Wilson, 2015), host numerous uranium prospects (Table 2). Known uranium occurrences are presently confined to the margins of the Eucla Basin where crystalline basement rocks are potential source areas for uranium (Fig. 1). Exploration for paleovalley-hosted uranium commenced in the mid-1970 s, initially focusing on the eastern Eucla paleodrainage, specifically the Kingoonya and Narlaby paleovalleys. This resulted in discovery of the Warrior and Ealbara prospects, both situated in tributaries of the Kingoonya paleovalley (Curtis et al., 1990), and four Yarranna prospects (up to 3550 ppm U_3O_8) in the Narlaby paleovalley and Yaninee prospect in the Yaninee paleovalley (Binks and Hooper, 1984). Uranium present in the eastern Eucla paleovalleys may have been sourced from Hiltaba Suite granites that are widespread on the Gawler Craton, variably weathered, and typically contain uranium contents 2–3 times above background levels. The eastern Eucla paleodrainage actively incised weathered basement during early to middle Eocene time with flow rates decreasing over time such that sandy valley fill and lignitic clays gave way, during Miocene time, to largely chemical carbonate sedimentation in a series of discontinuous lakes strung out along the major drainage lines (e.g., Hou et al., 2007b). Anomalous levels of uranium have been reported also in other paleodrainage networks, including the Woldra paleovalley

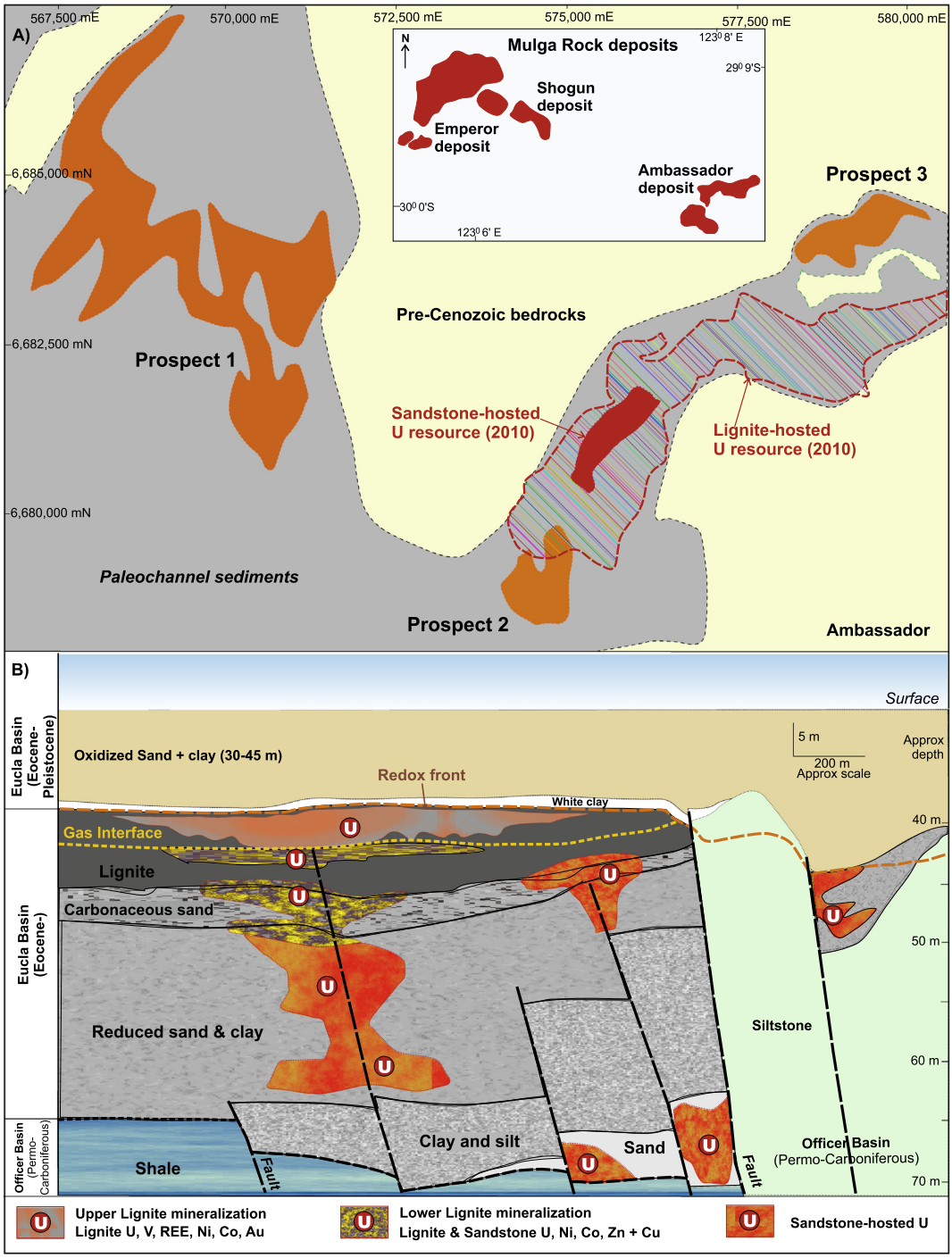

Fig. 9. Uranium deposits/prospects (A) and schematic section of the stratigraphy and mineralization types at Ambassador (B) through Mulga Rock uranium area (for the location see Fig. 1C) (modified from Inwood, 2009; Energy and Minerals Australia, 2010).

and Lake Bring estuary (16 to 643 ppm U_3O_8) (Curtis et al., 1990) and the Thurlga paleovalley (8 m at 106 ppm U_3O_8) (Adelaide Resources, 2009).

Paleovalleys along the western margin of the Eucla Basin drain potential uranium source rocks of the Yilgarn province. Uranium discoveries within this drainage network include the Mulga Rock and Ponton uranium deposits where extensive drilling has been undertaken in recent years (Penney, 2012). These uranium deposits lie within the Raeside paleovalley system, which incised deeply weathered crystalline rocks of the Yilgarn Craton and Albany-Fraser Province and can be traced for more than 100 km across the western Eucla margin and eastern Yilgarn Craton. The Mulga Rock uranium deposits are characterized by numerous mineralized zones within interbedded sand and lignite (see 'Lignite deposits' below), which are hosted by middle Eocene sediments within a sequence of up to 100 m of Paleogene fluvial, estuarine and lacustrine sediments that overlie preserved remnants of Cretaceous and Permian sediments (Macfarlane and Inwood, 2010). Drilling at Mulga Rock has outlined four separate deposits, Ambassador, Shogun, Emperor and Princess. The Ponton deposits, containing eight

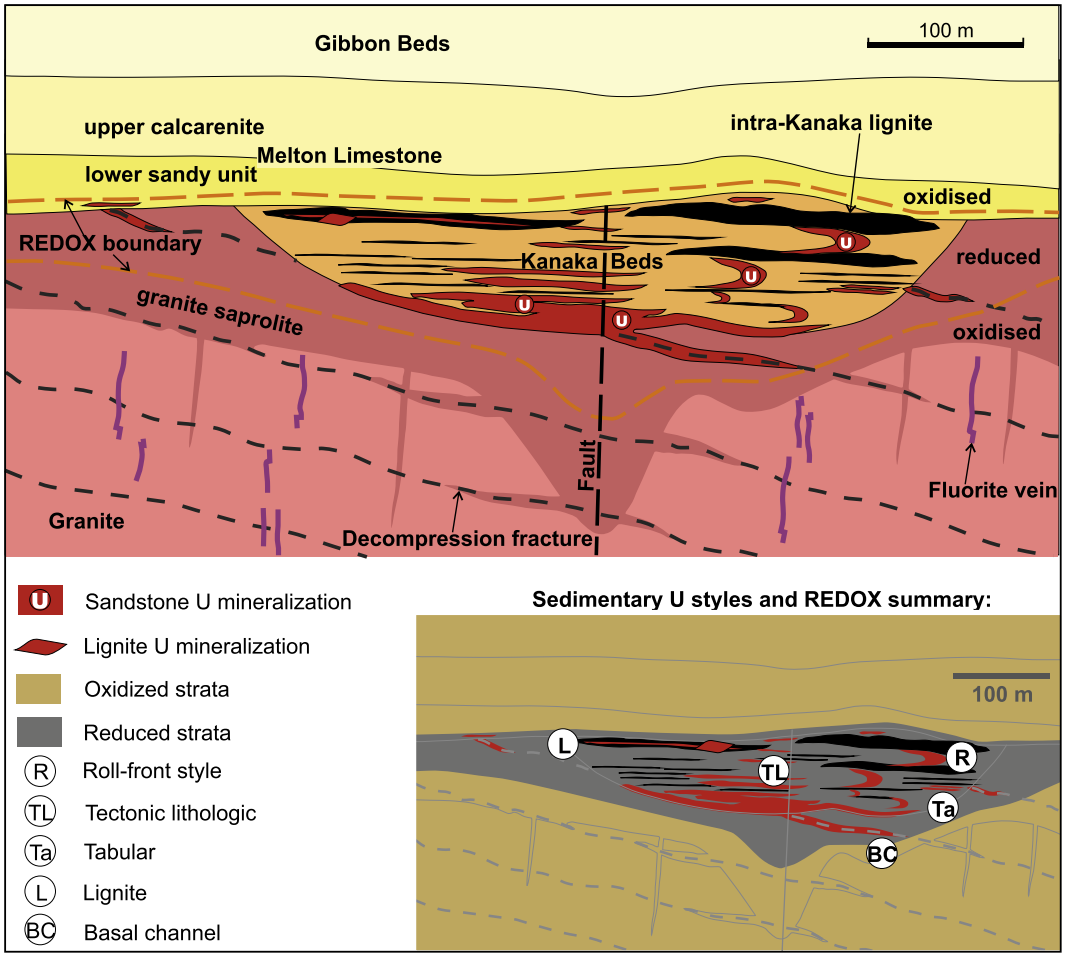

Fig. 10. Geological cross-section through Blackbush uranium deposit, Pirie Basin, South Australia (for the location see Fig. 1A) (after Hou et al., 2014).

prospects are hosted in the same paleodrainage network as Mulga Rock (~25 km to the south) (Fig. 9).

2.4.4. Pirie Basin, South Australia

Exploration in the Cenozoic paleovalleys of the Pirie Basin resulted in the greenfield discovery of Blackbush and Plumbush deposits in 2007 (Fig. 1; Table 2). The uranium mineralization (coffinite and uraninite) at Blackbush (inferred resource of 63 million tonnes at 0.029% eU_3O_8 containing 18 300 tonnes U_3O_8, at cut-off grade of 0.01% eU_3O_8) (Bluck, 2009a,b, Uranium SA, 2013) is hosted within a Cenozoic sand unit, at and below the contact between carbonaceous to lignitic mature, monomictic sand units of Eocene age (Kanaka Beds) and an overlying oxidized, mature, polymictic sand unit of Miocene age. The U-bearing paleovalleys include channels that incise bedrock of weathered Hiltaba suite granite that is locally enriched in uranium and recognized throughout the region as a potential uraniferous source rock. The significance is that several different types (e.g., roll-front, tabular, basal channel, techonic-lithologic, and lignite) of the paleovalley-related uranium orebodies can be observed within a single paleovalley system (Fig. 10). The thicker and higher grade zones in the sediments appear to track along the deeper parts of the paleovalleys (up to 26.5 m at 0.19% eU_3O_8; Bluck, 2009a,b, Uranium SA, 2013). Uranium mineralization at Blackbush and Plumbush together with prospects Sugarbush and Emubush make up the Samphire uranium project. These recent discoveries of paleovalley-hosted uranium within the eastern Gawler Craton region of South Australia significantly upgrade the exploration potential of this region for further discoveries of paleovalley-hosted uranium mineralization.

2.4.5. Ordos Basin, north China

The Ordos Basin is a Mesozoic intracontinental basin developed on the Paleozoic sedimentary rocks that in turn are underlain by Precambrian basement of the North China Craton (Fig. 11). The basin (~370,000 km^2) is surrounded by the highland basement rocks of Luliang and Zhongtiao Mountains in the east, Helan and Liupan Mountains in the west, Lang, Yin and Daqing Mountains in the north, and Qinling Mountain in the south. These basements are composed of Archean and Lower Proterozoic metamorphic rocks, including granite gneiss, amphibolite, and granites with relatively high uranium contents. Discovery of the sandstone uranium deposits in the early 2000s ensured the Ordos Basin became a more important energy resource region, in addition to the oil-gas and coal resources (Li et al., 2008).

Uranium mineralization occurs in the margins of the basin (e.g., Dongsheng deposits including Sunjialiang, Zaohuohao, Shashagetai and Daliuta sub-deposits in the north margin; and are mainly hosted in reduced (grey-green and grey) sandstones of the middle Jurassic Zhiluo Formation, which were deposited in Jurassic braided channels (Fig. 11) (Li et al., 2005, 2007b; Cai et al., 2007a, b). Uranium (mainly coffinite) is concentrated in the transitional zones between grey-green and grey sandstones of the Zhilou Formation of Middle Jurassic age, in similar manner to those of the Monument Valley and White Canyon districts, USA, which were

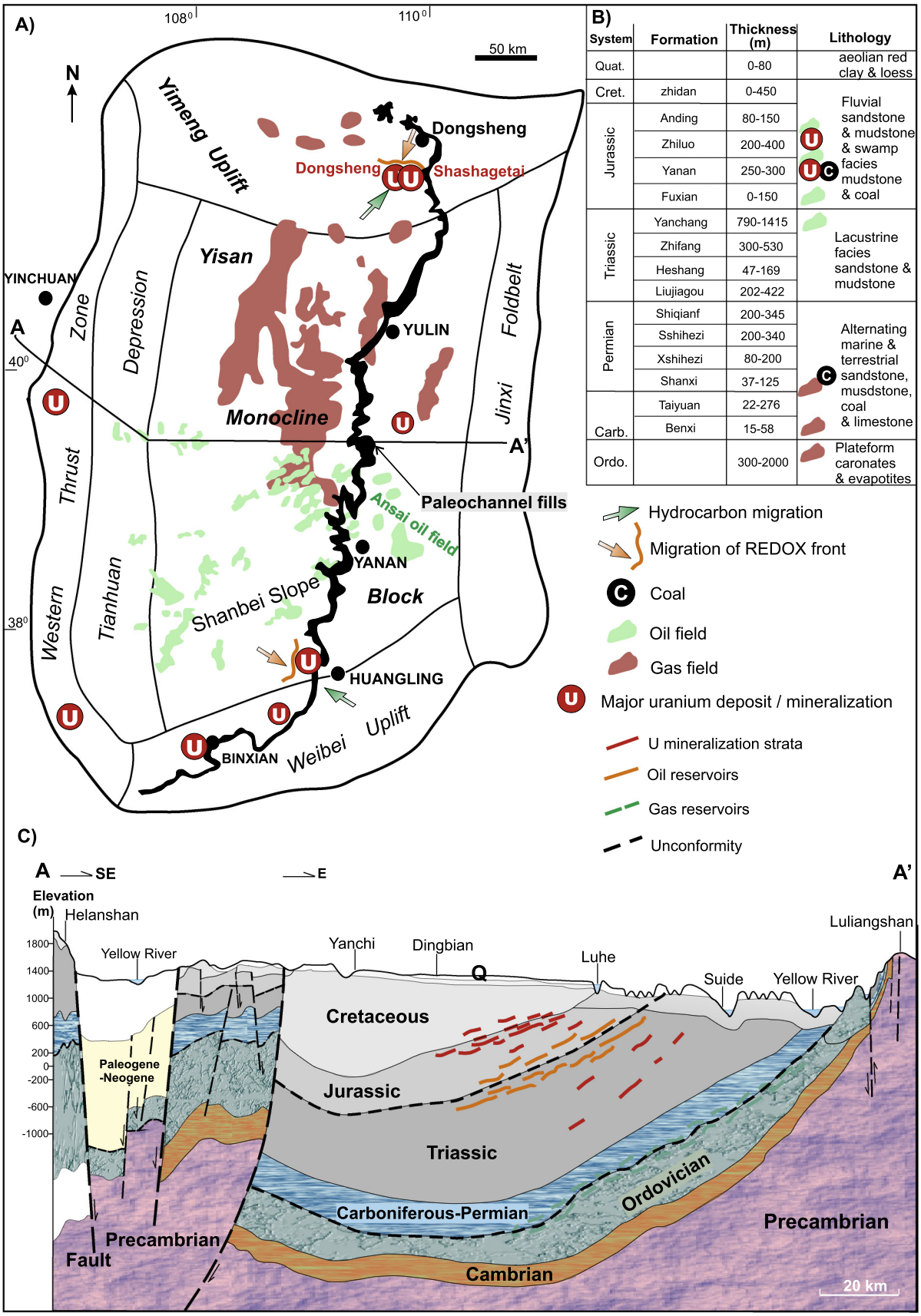

Fig. 11. Map and figures of Ordos Basin, north China (for the location see Fig. 2), showing major paleovalley-related uranium deposits (A), representative stratigraphy (B), cross-sections of the basin (C), tabular to rollfront uranium mineralization (D) and U-bearing units (E) in the Dongsheng deposit, and mineralizing model (E) (modified from Cai et al., 2007a, b; Li et al., 2008; Hou et al., 2014).

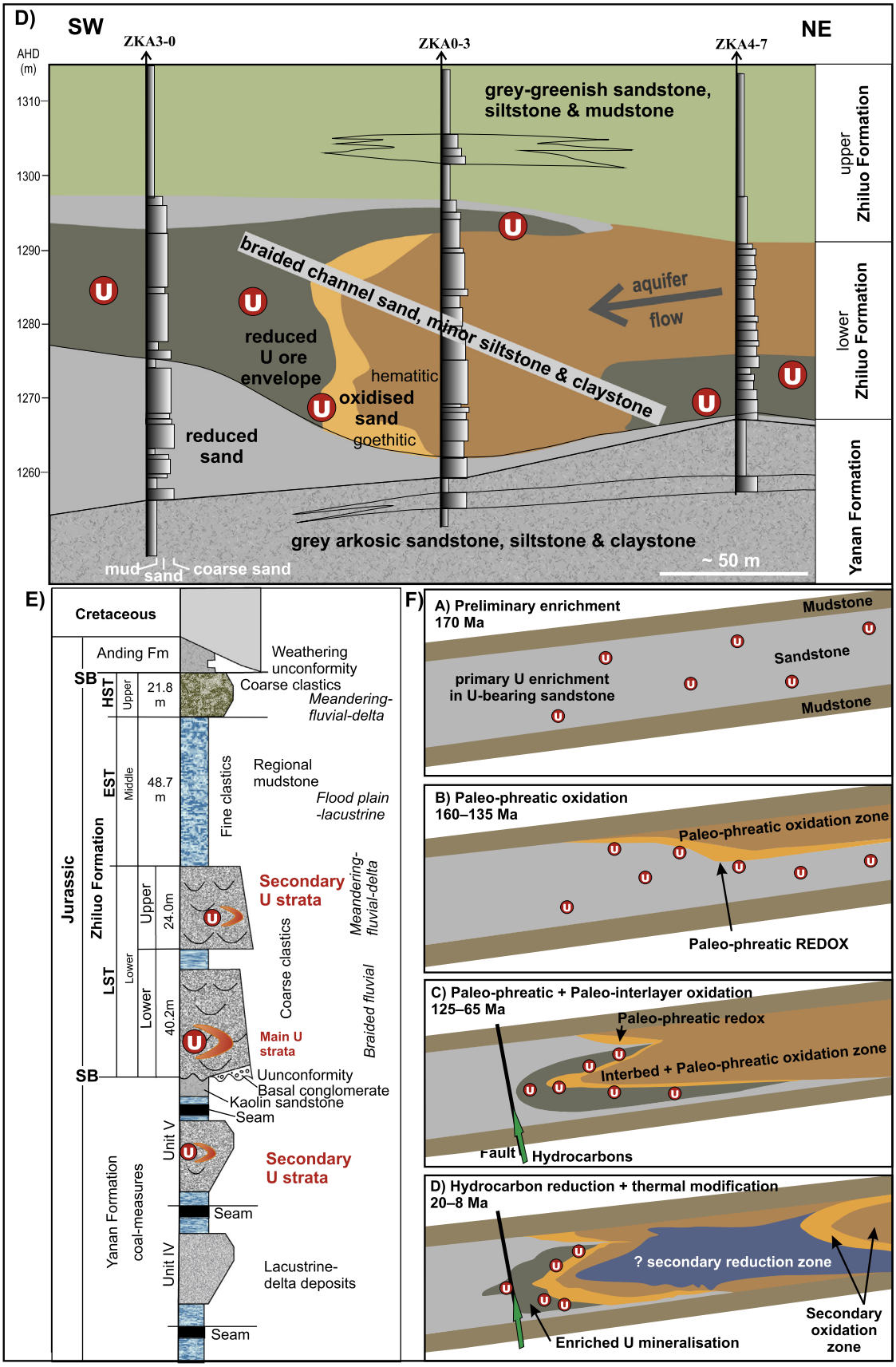

Fig. 11 (*continued*)

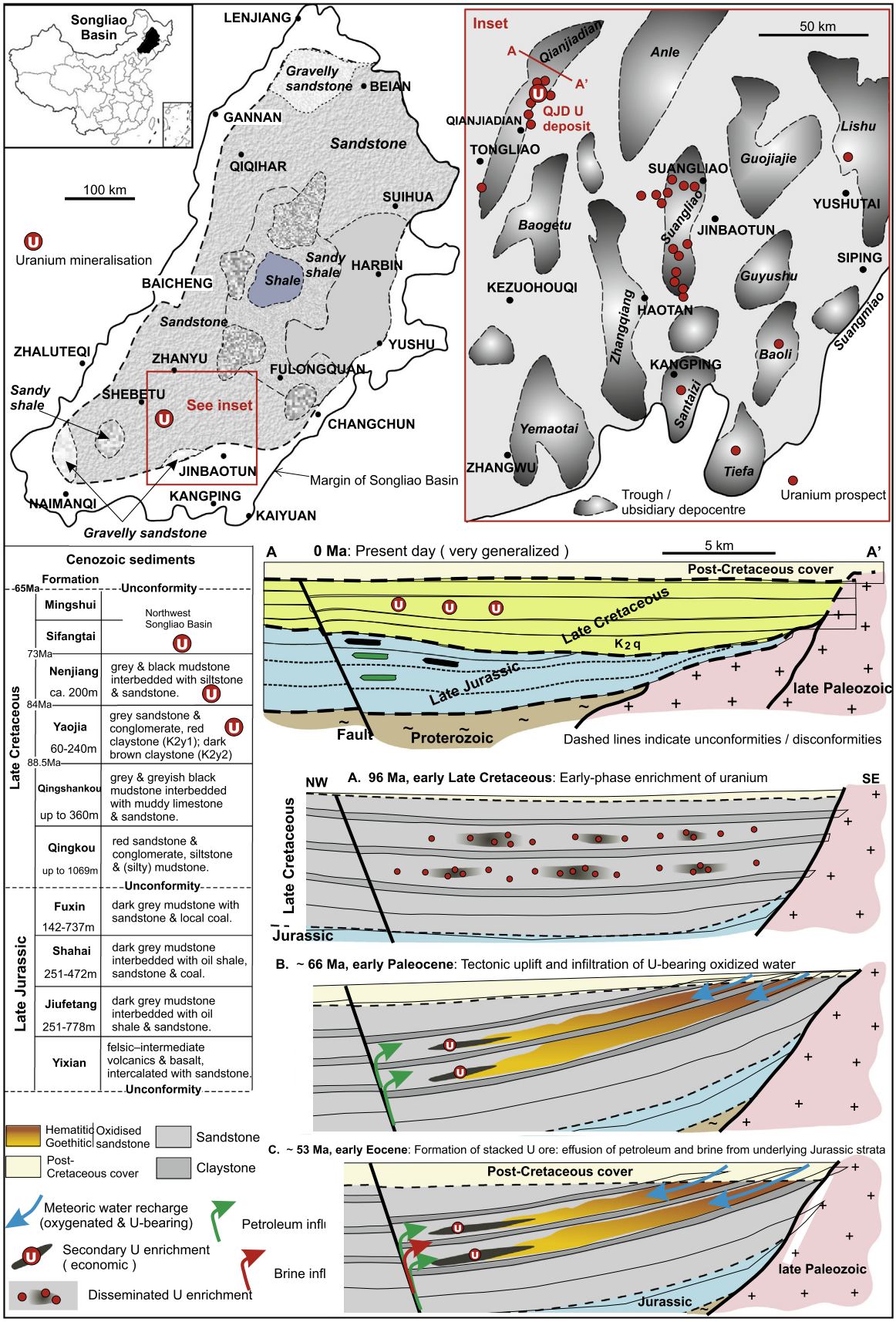

Fig. 12. Maps and figures of major uranium deposits and prospects in subsidiary depocentres along the western and southern margins of the Songliao Basin (for the location see Fig. 2), northeastern China, showing representative stratigraphy, and Palinspastic cross-section model and mineralized model for the formation of QJD uranium deposits: Stage A: Pre-enrichment of uranium in the Yaojia Formation; Stage B: Tectonic uplifting and infiltration of U-bearing oxidized water; Stage C: Effusion of petroleum (oil + gas) and brine into Cretaceous strata (modified from Li et al., 2008; Shi et al., 2012; Feng et al., 2014; Hou et al., 2014).

deposited in late Triassic braided and meandering channels (Dahlkamp, 1993). Geologic and geochemical characteristics of the uranium deposits in the Ordos Basin indicate that uranium mineralization resulted from mixing between uranium-bearing, oxidizing fluids and hydrocarbon-carrying, reducing fluids (Xue et al., 2010). Individual orebodies of the Dongsheng deposits generally extend from 3 to 8 m (up to more than 20 m) in thickness, several hundred to 1000 m in width, and several to more than 10 km in length along the paleovalleys. The ores, mainly composed of coffinite, are typically low- to medium-grade, commonly ranging from 0.03 to 0.5% U_3O_8, but locally can be as high as 2.4% U_3O_8. In the Dongsheng area, the ages of uranium mineralization (U–Pb isochron method) range widely from 177–149 Ma, 124–107 Ma, 85–74 Ma and 20–8 Ma, but are concentrated in the Late Cretaceous (Xia et al., 2003a; Liu et al., 2007). Near the front of the roll-shaped orebodies, the main mineralization shows younger U–Pb ages, ranging from 20 ± 2 Ma to 8 ± 1 Ma (Xia et al., 2003b). These ages are very similar to those reported for other U deposits in Yili and Tuha basins, NW China (see below; Min et al., 2005a).

As in the Beverley deposit of South Australia, the interface of oxidized and reduced phases is not obvious in the uranium deposits of the Ordos Basin. The greenish color is thought to result from secondary oil-gas reduction process, and is due to acicular-flakey chlorite coating the surfaces of sand grains (Li et al., 2008). Extrinsic reductants emanating from deeper oil and gas reservoirs have been proposed also as a source of reductants for giant sandstone-hosted uranium deposits in Kazakhstan (Jaireth et al., 2008). The critical components needed to precipitate and concentrate uranium require multiple sources including the surrounding Archean-Early Proterozoic basement and Mesozoic uranium-bearing strata, and oil-gas fluids. These came together to form uranium deposits during several recognized mineralizing processes and in stages, recognized as tectonic 'dynamic-static' coupling movements, superposition of paleo-phreatic oxidation and interlayer oxidized mineralization, and composite transformation of oil-gas and thermal fluids, as shown in Fig. 11.

2.4.6. Songliao Basin, northeast China

The Songliao Basin, containing a number of NNE-SSW oriented sub-basins, is located at the eastern edge of the Central-Asia Uraniferous Province (Fig. 2). Songliao Basin is a large Mesozoic-Cenozoic terrestrial sedimentary basin surrounded by several mountain ranges, including the Zhangguangcailing, Daxinganling, Xiaoxinganling and Gutiefaqiuling ranges (Shi et al., 2012); over 11 major paleodrainage systems drained these highlands and discharged into the central basin during Cretaceous time (Pan et al., 2011). The uranium mineralization, controlled by the deep faults, mainly occurs in late Cretaceous meandering and/or braided fluvial sediments and (Fig. 12) (Feng et al., 2014; Li et al., 2008). In the western Songliao Basin the sandstone uranium mineralization is mainly hosted in Sifangtai (K_2s) and Nenjiang (K_2n) formations and the characteristics of these paleovalley related uranium deposits are similar to those in Bayanwula area, Erlian Basin (see below) (Feng et al., 2014). In the southern Songliao Basin, however, the sandstone uranium mineralization is mainly hosted in Yaojia (K_2y) Formation (Li et al., 2008).

The QianJiaDian (QJD) uranium deposit is located in the QJD fault-controlled sub-basin (sag) within the southwestern Songliao Basin, Inner Mangolia. Here, the tabular uranium deposits are hosted in channel sediments of the late Cretaceous Yaojia Formation (K_2y) (Fig. 12), but the mineralizing age of QJD uranium deposit is about 53 ± 3 Ma, suggesting an epigenetic mineralization (Feng et al., 2014; Li et al., 2008). The host Yaojia Formation, mainly consisting of reddish thick (medium-fine-grained) sandstone, siltstone and thin mudstone layers, was reduced and altered due to migration of organic fluids emanating from deeper in the basin, resulting in the grey to light grey ore-bearing host rocks. These rocks are vertically graded and form a typical braided fluvial facies. The sandstones near redox zones in these sandstone-hosted uranium deposits often contain calcite cement with light carbon isotope ($\partial^{13}C = -6.8‰$), indicating that the source of carbon was organic produced by anaerobic bacteria (Dong et al., 2005). The formation of these uranium deposits resulted from four stages (Li et al., 2008): 1) initial enrichment of uranium during deposition of Yaojia Formation braided channel sediments; 2) tectonic uplift and infiltration of U-bearing oxidized water; 3) effusion of oil-gas and brine through faults; and 4) alteration of sand bodies under conditions of good permeability and abundant reduced matter (Fig. 12).

2.4.7. Erlian Basin, north China

Erlian Basin is an intracontinental basin of northeastern China developed from Late Jurassic (*syn*-rift stage dominated by lacustrine deposits) to Late Cretaceous (post-rift stage dominated by fluvial and shallow lacustrine deposits), and is composed of five major sub-basins framed by a series of ENE–WSW oriented horsts or ranges (Fig. 13A) (Dou and Chang, 2003; Dou et al., 1998; Wei et al., 2005 Fan et al., 2008; Nie et al., 2007). The post-rift stage Erlian Basin is characterized by the deposition of Late Cretaceous Saihan and Erlian formations (Fig. 13B), in which sandstone layers consist of amalgamated channels or sandy bedforms of braided river systems alternating with more or less continuous mudstone layers of overbank deposits (Bonnetti et al., 2014). It is this alternation that is favorable for forming tabular and/or roll front-type uranium deposits in confined permeable sandstone layers. In the Erlian Basin, permeable and reduced sandstone layers confined between aquitards, are sites of sandstone-hosted uranium (e.g., Nuheting and Bayinwula) deposits in the braided fluvial systems of post-rift sediments of the Erlian Basin (Fig. 13B). These post-rift sediments may also originally have contained significant synsedimentary to diagenetic uranium mineralization that was a possible uranium source for the formation of roll front mineralization (Bonnetti et al., 2014). Significant synsedimentary pre-concentrations of uranium (mainly adsorbed on clay minerals within the post-rift sediments) were redistributed essentially *in situ*, during the diagenetic evolution of the sediments, to form a mineralization consisting of coffinite and uraninite replacing pyrite or pyritized organic matter (Bonnetti et al., 2015a, b).

The Bayinwula deposit is located in the western part of the Manite sub-basin, about 100 km to the east of Erlian city, Inner Mongolia (Fig. 13A). The Bayinwula roll front-type (Fig. 13B) uranium deposit is mainly hosted in braided channel (reduced) sandstone layers (gravel and very coarse to fine-grained sands) of the upper member of Saihan Formation, which are typically intercalated with thin overbank-distal floodplain silts, clays and coal strata (Fig. 13B) (Nie et al., 2007; Fan et al., 2008), and is characterized by a dominantly biogenic model involving reactions between organic matter, U-rich Fe/Ti oxides and sulfate-reducing bacteria (Bonnetti et al., 2014). The Bayinwula deposit, situated at between 100 and 160 m below the surface, is composed of three main orebodies, which extend over 7 km along the redox front and are a few hundred meters wide (Nie, 2008). The uranium mineralization (generally low grade at a mean of 100 to 300 ppm U) is hosted in medium- to coarse-grained sandstones, rarely fine-grained, and mainly occurs as coffinite associated with pyrite and organic matter (Bonnetti et al., 2015b). The uranium mineralization contained in the primary reduced sandstone was mostly accumulated by remobilization during secondary oxidation (Bonnetti et al., 2015b). Uranium contained in Fe/Ti oxides and organic matter is liberated and leached by oxygenated groundwater, and subsequently precipitated by H_2S reduction at the redox front as P-rich

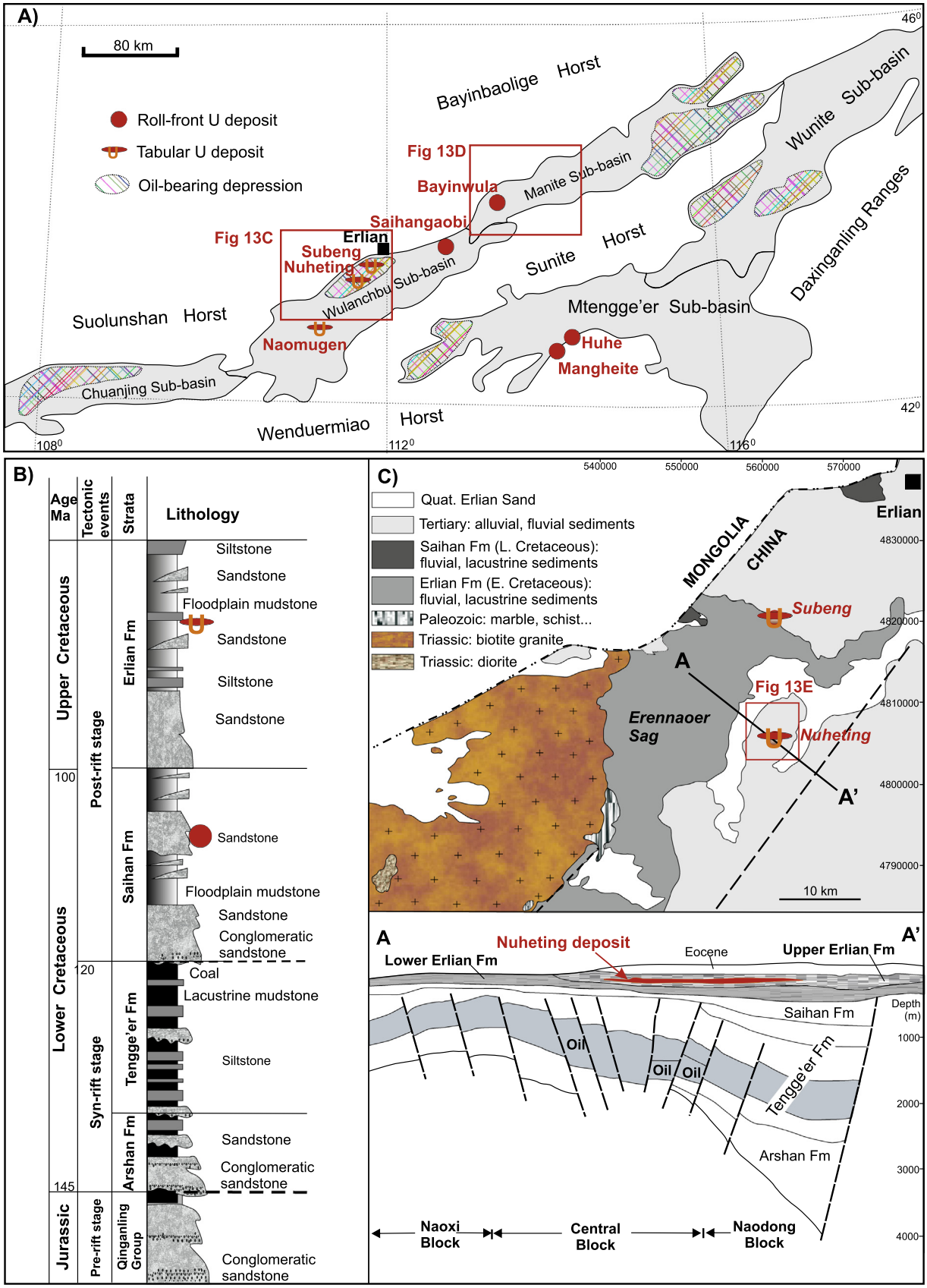

Fig. 13. Maps of Erlian Basin (A), for the location see Fig. 2); representative stratigraphy (B); Wulanchabu Sub-basin and cross-section (C); showing geology, structure, uranium deposits, oil-bearing depressions, and location of cross-sections presented in Fig. 13B. For the location see Fig. 2. Modified after CNNC (unpublished data), Dou et al. (1998), Meng et al. (2003) and Wei et al. (2005), Dahlkamp (2009), and Bonnetti et al. (2014). Fig. 13D of Bayinwula Deposit area and Roll-front uranium enriched cross-section; E) Nuheting uranium deposit area (topography) and cross-section; F) mineralizing model of Erlian Basin (modified from Dou et al., 1998; Bonnetti et al., 2014; Bonnetti et al., 2015a,b). For the location of drillholes and cross-sections see Fig. 13A.

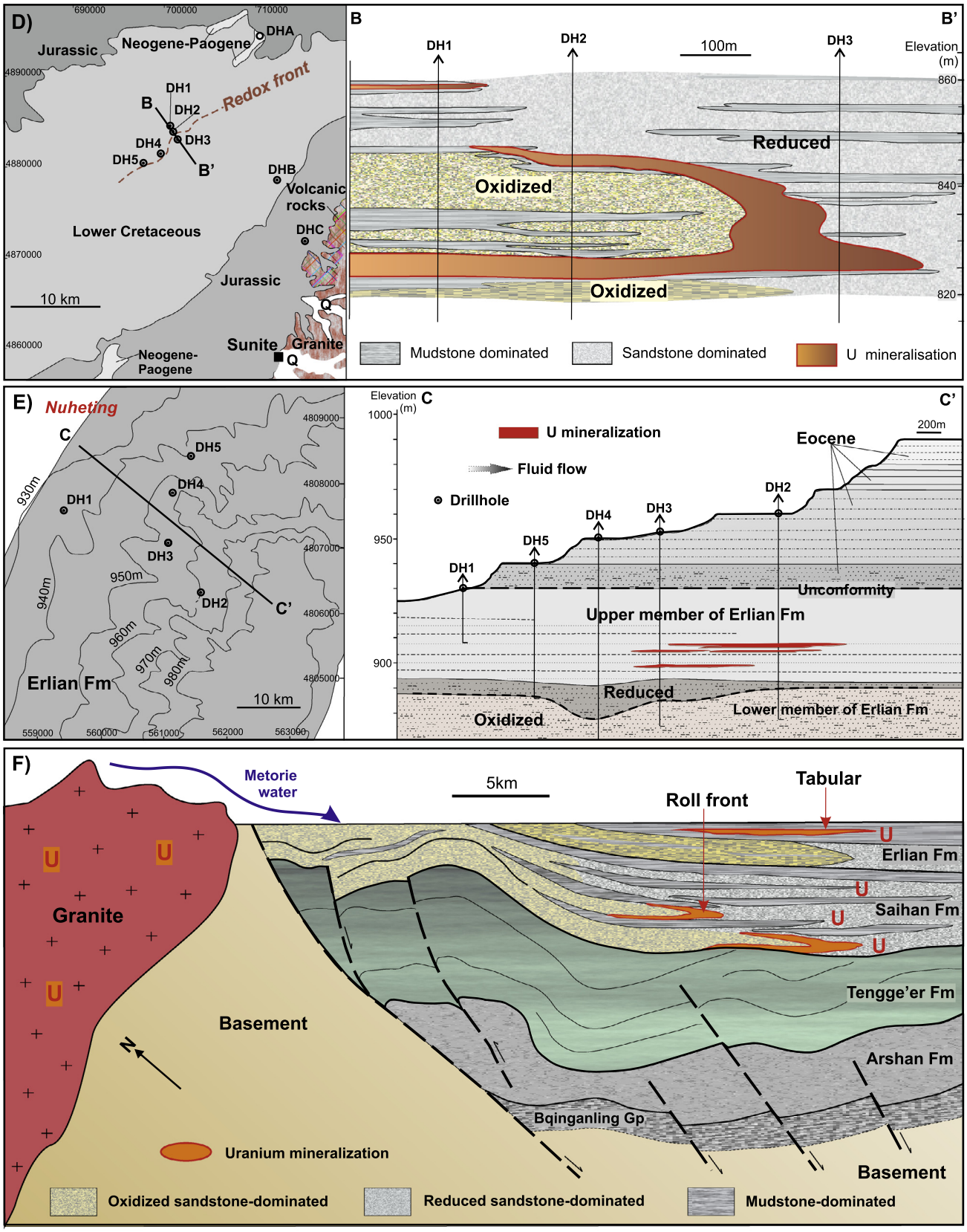

Fig. 13 (*continued*)

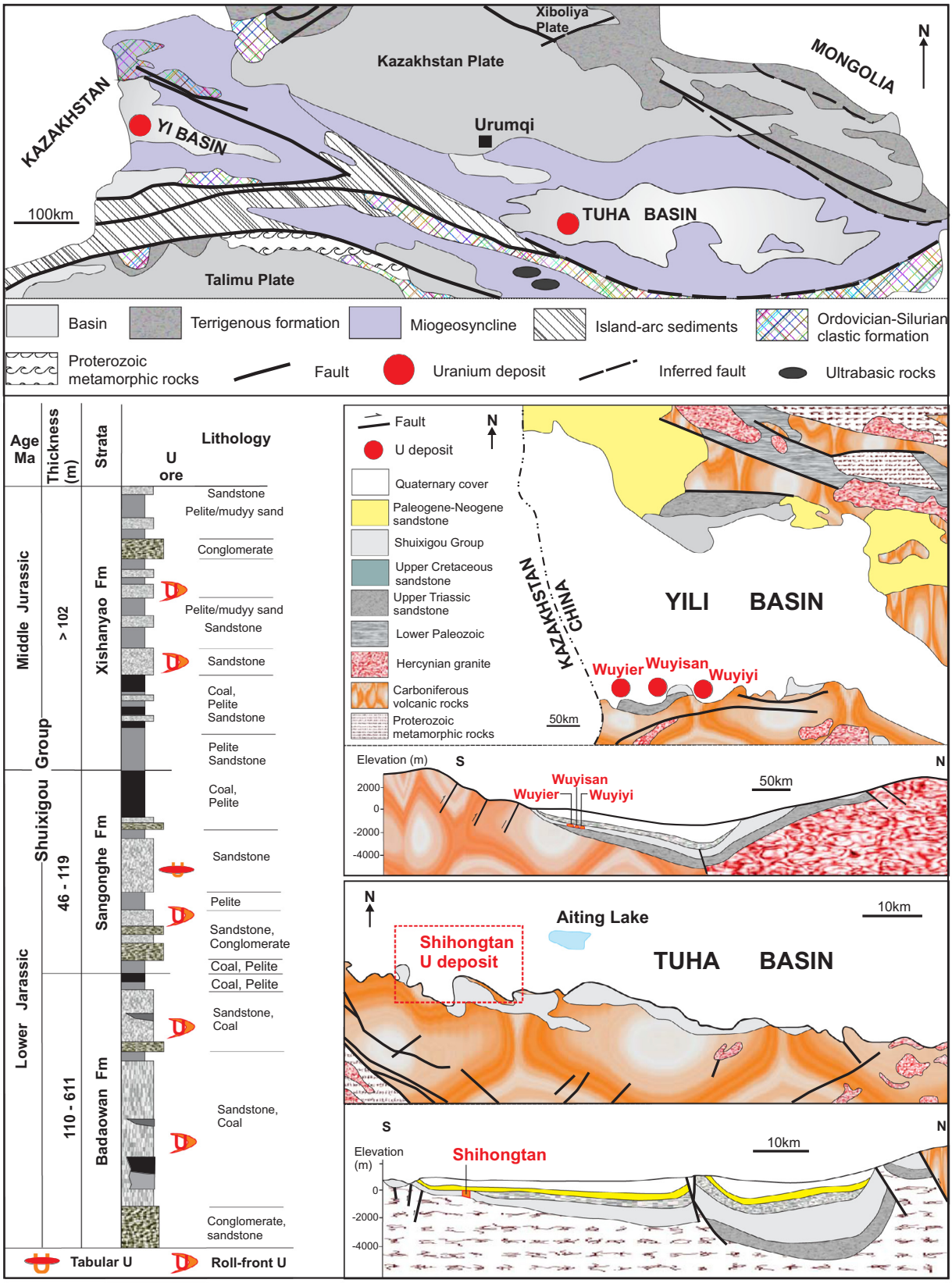

Fig. 14. Simplified maps of the Yili Basin (Wuyier, Wuyisan, and Wuyiyi deposits) and Tuha Basin (Shihongtan U field), NW China, showing geology, stratigraphy and uranium deposits. For the location see Fig. 2 (modified from Chen et al., 2000; Min et al., 2001, 2005).

Table 3
Mulga Rock-Ambassador uranium deposits. Inferred resource as of 2009 June 2010. Reported by host type using a lower cutoff of 200 ppm U_3O_8 assuming open cut mining. Ordinary Kriging Grade Estimates within Parent Cells of 200 m by 100 m by 10 m. Using Cut comb U_3O_8 Composites (combined chemical and radiometric grades) (from Coffey Mining Pty Ltd, 2010).

Host Type / Lithology	U_3O_8 Grade (ppm)	Tonnes (Mt)	Contained Metal(Kt U3O8)
Upper Lignite – Lignite and carbonaceous claystone	600	16.7	10.0
Lower Lignite/Sandstone – Mixed environment of lignite, carbonaceous sandstone and sandstone	320	3.7	1.2
Sandstone – Reduced sandstone	310	4.0	1.2
Total	510	24.4	12.5

coffinite and ningyoite ($(U,Ca,Ce)_2(PO_4)_2.1\text{-}2H_2O$) (Bonnetti et al., 2014).

The Nuheting deposit (estimated resources > 10,000 t U at a grade ranging from 0.03 to 0.1% U; Dahlkamp, 2009) is hosted in the Late Cretaceous Erlian Formation (Fig. 13B), in the Erennaoer Sag of the Wulanchabu Sub-basin (Fig. 13A) (Li and Kuang, 2010). In the area of the Nuheting deposit, the Erlian Formation is about 50 m thick and divided into (i) sandstone-dominated lower member (K_{2e1}) of braided channel deposits, and (ii) mudstone-dominated upper member (K_{2e1}) of overbank deposits that host the Nuheting deposit (Bonnetti et al., 2014). In contrast to several lower sporadically distributed small ore bodies, the upper main ore body (8.5 km long by 1.0–3.5 km width and 0.7–1.3 m thick; CNNC, unpublished data; Dahlkamp, 2009) is shallow, blanket shaped, and located at the top of the mineralized sequence, and represents more than 90% of the total uranium resources. The tabular-type uranium mineralization of the Nuheting deposit is mainly hosted in pyrite-and organic matter-rich, dark-grey silty mudstones (with a minor proportion occurring in siltstone and sandstone; Yan et al., 2010) of wetland depositional environments that usually correspond to favorable reduced environments for the concentration of uranium during synsedimentary/early diagenetic stage (e.g., Otton, 1984; Cuney and Kyser, 2008; Dahlkamp, 2009; Douglas et al., 2011). Most of the uranium mineralization in the Nuheting deposit appears to be facies-controlled, mainly hosted in organic matter-and pyrite-rich dark grey silty mudstone (~52%), siltstone (~37%), sandstone (~7%), and calcareous mudstone (~0.5%) (Yan et al., 2010). Bonnetti et al. (2015a) concluded that the Nuheting deposit developed over three main stages: 1) synsedimentary/early diagenetic uranium concentration and mineralization, 2) late diagenetic *in situ* uranium remobilization and deposition on pyrite, and 3) epigenetic cementation.

2.4.8. Yili and Tuha Basins, northwest China

Paleovalley-related uranium deposits occurring within the Xinjiang uranium province include Wuyier, Wuyisan and Wuyiyi deposits that are located in Yili Basin (Mesozoic) close to the borders of Xinjiang and Kazakhstan, and Shihongtan deposit that is situated in Tuha Basin (Mesozoic), the eastern extension of the Kazakhstan–Uzbekistan U-province (Fig. 14) (Chen et al., 2000). These two continental basins, also host several large oil and natural gas reservoirs as well as coalfields, and overlie bedrock of Proterozoic metasedimentary units, Carboniferous intermediate, acidic volcanic and volcaniclastic rocks, and granites of Hercynian age, which are considered the source of the sediments and the uranium (Min et al., 2005a).

The roll-front/tabular uranium mineralization, located in the southwest margins of both basins (Fig. 14), is hosted in Lower–Middle Jurassic coarse- to medium-grained sandstones (alluvial fan-braided stream facies; with minor amount of uranium hosted within mudstone and coal) of Shuixigou Group that comprises three (Badaowan, Sangonghe and Xishanyao) formations, which are characterized by dark grey to black colors due to a mixture of ore minerals and (2–3%) carbonaceous debris (Min et al., 2005a). The paleovalleys that host alluvial fan-braided stream facies typically extend over 100 km long and are up to 20 km wide (Min et al., 2005a). The gently dipping ore (uraninite and coffinite)-bearing sandstones are generally bounded by impermeable mudstones. Multiple generations of sulfide minerals, including pyrite, marcasite, sphalerite and galena, are largely in textural equilibrium with the uranium minerals. Some of the roll-front ore bodies (commonly 4 to 10 m in thickness and 50 m in length) occur along single or double C-shaped roll-type surfaces or envelopes, representing interfaces between oxidized-altered rock and reduced-unaltered rock; whereas the tabular ore bodies (generally 3–18 m in thickness and 200 m in length) are usually parallel to bedding (Min et al., 2005a). In contrast to the host-rocks, the much younger U–Pb ages (11.7 ± 0.3 Ma to 15.8 ± 0.4 Ma) of U-mineralization corresponds with the timing of Himalayan (Neogene) tectonism that affected a vast region of NW China (Min et al., 2001), suggesting epigenetic processes of mineralization were initiated by tectonically-induced fluid movement.

2.5. Lignite-hosted deposits

Uranium mineralization occurring in lignite or coal immediately adjacent to carbonaceous mud and silt/sandstone beds, commonly with high pyrite content, are known from several sites worldwide including the Serres Basin, Greece, North and South Dakota (USA), Springbok Flats (South Africa), Nizhneylyiskoye (Kazakhstan), and Freital (Germany) but uranium grades are typically very low and average less than 0.005% U_3O_8 (McKay and Miezitis, 2001). Uranium adsorbed on carbonaceous matter is not present as discrete uranium minerals. The uranium associated with this type of mineralization was generally consider too low grade to be of commercial interest (Dahlkamp, 1993), but higher grade deposits have been reported subsequently, in Australia (e.g., Mulga Rock deposits, Table 3) and China (e.g., Erlian and Ordos basins described above). Lignite style uranium mineralization at the Ambassador deposit, Mulga Rock of Western Australia includes upper and lower lignite zones with associated sandstone-hosted uranium mineralization (Macfarlane and Inwood, 2010). This interbedded feature of the sandstone-hosted and lignite-hosted uranium mineralization in a deposit enhance the economic significance of the deposit relative to simply lignite-hosted uranium mineralization.

The *Mulga Rock deposits*, comprising three separate zones of mineralization, Shogun, Emperor and Ambassador, are situated in the western margin of the Eucla Basin (Clarke et al., 2003), approximately 250 km east-northeast of Kalgoorlie in Western Australia (Fig. 1). The deposits are distributed along the outer margin of a broad bend in a Cenozoic paleovalley that is 5 km to 15 km wide and over 100 km (traced, and likely extended over 400 km) in length draining the Yilgarn Craton from NW to SE (Douglas et al., 2003; Inwood, 2009) and discharging into the Eucla Basin (Clarke, 1993; Clarke et al., 2003). The uranium mineralization is hosted by lignite, carbonaceous clay and sand. Highest grades, average 0.06% U_3O_8, are in lignitic clays immediately below the redox boundary at the base of the weathered zone (Macfarlane and Inwood, 2010). The mineralized zones are characterized as tabular, roll-front and basal-channel, averaging about 2 m thick, are flat-lying and are from 20 to 50 m below surface (Fig. 9). The redox boundary (commonly > 30 m deep) presents as a sharp front between kaolinitic paludal clay and lignite and commonly

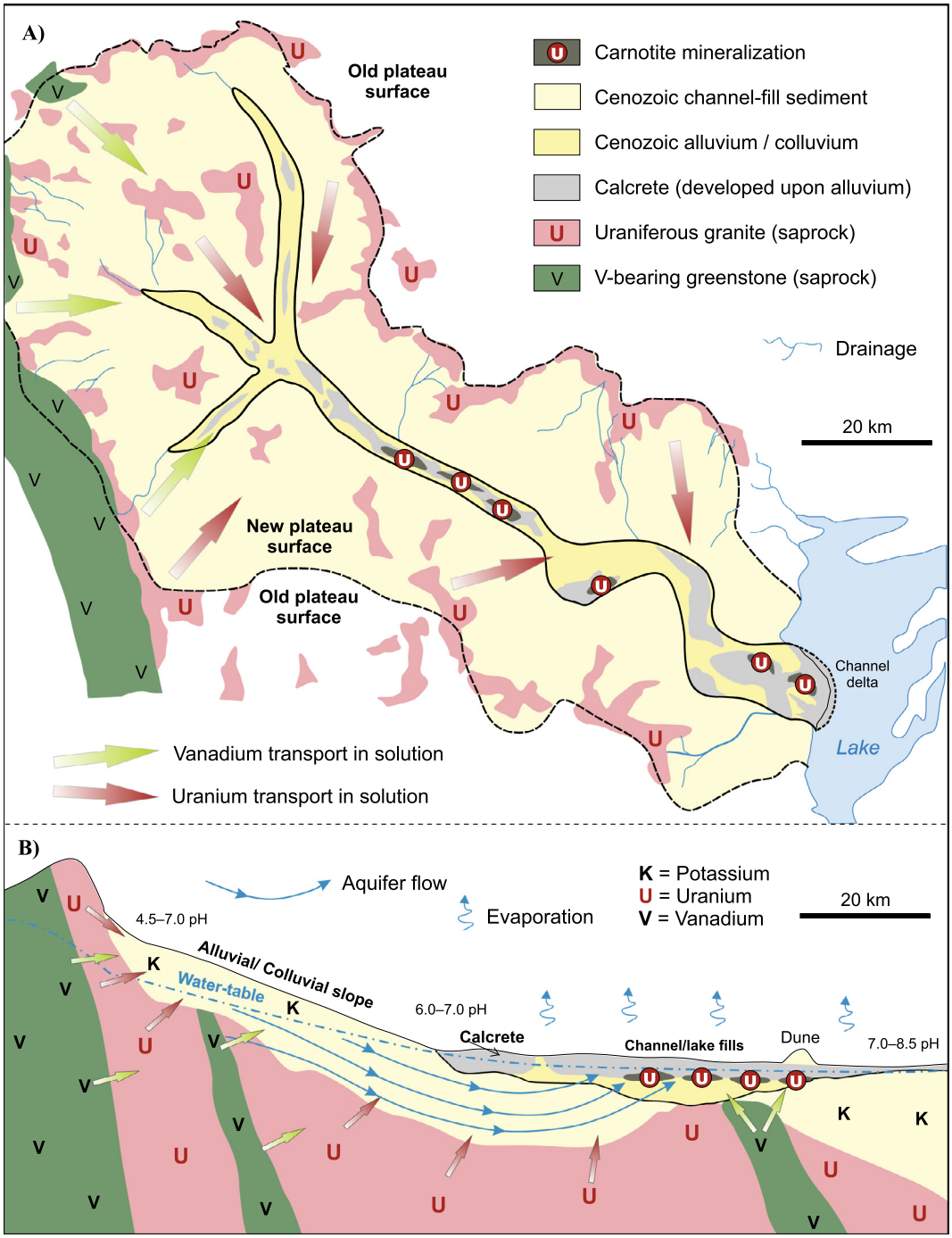

Fig. 15. a) Generalised model of valley-fill calcrete-hosted (carnotite) uranium mineralization, based on Yeelirrie and Lake Way deposits, Western Australia; b) Schematic cross-section through calcrete-hosted uranium mineralization model, based on Yeelirrie and Lake Way deposits (modified after Mann and Deutscher, 1978; Cameron, 1990).

approximates the present day water-table (Douglas et al., 2003; 2011). The channel sediments were deposited during middle Eocene time and are composed of three broad units (Fig. 9): 1) basal fluvial sands and gravels; 2) lacustrine to paludal sediments, including lignite, clay-rich lignite and carbonaceous sands; and 3) fluvial sands and interbedded lacustrine sediments, which are generally oxidized, ferruginized and silicified (Douglas et al., 2003; 2011).

Three major styles of uranium mineralization are recognized at the Ambassador deposit, Mulga Rock (Macfarlane and Inwood, 2010): 1) Upper Lignite - enriched in U, REE, Ni, Co, Sc, V and locally Cu and Ag; 2) Lower Lignite and associated sandstone; also enriched in base metals; and 3) a basal sandstone hosted mineralization. Uranium and other metals (e.g., Cu, Ni, Co, Se, Pb) were first concentrated syngenetically within reduced sediments (e.g., peat-derived lignite, clay-rich lignite and carbonaceous sands and clays; Douglas et al., 2003, 2011) and are mainly associated with organic matter or clay minerals. Macfarlane and Inwood (2010) consider that the metals probably migrated upwards along fault zones, through the sandstone and lignite, finally being trapped by an impervious clay layer overlying the lignite.

Uranium, sourced from granitoids and metamorphic rocks of the Yilgarn and Albany-Fraser Provinces, was transported along with detritus forming the paleovalley sediments and adsorbed

onto organic matter within the lignite/carbonaceous clay (Fulwood and Barwick 1990). As for the Nuheting deposit, this synsedimentary concentration was likely remobilized and concentrated within the host-lithologies (tabular-shaped uranium mineralization mainly in lignite, roll-front and basal-channel mineralization mainly in lignitic sands; Fig. 9) during diagenesis and then further remobilization by later oxidizing groundwater circulation through permeable sandstones either at the top or the base of the enriched, reduced lithologies. This had the effect of upgrading the initial low concentration of uranium. The grade of mineralization and thickness are controlled by permeability and organic matter-content of the host sediments, with the highest grades and thickest zones of mineralization developed within the more organic-rich and more permeable sediments (Macfarlane and Inwood, 2010). Oxidized sands and silts above the redox boundary are depleted in uranium relative to daughter products, whereas reduced sediments immediately below the redox boundary are enriched in uranium relative to daughter products (Fulwood and Barwick, 1990).

2.6. Calcrete-hosted (surficial) deposits

Calcrete-hosted uranium deposits appeared in the Cenozoic when valley calcretes were formed under relatively arid climatic conditions, with shallow groundwater drainage of low topographic gradients ~1% (10 m/km; Karner and Becker, 2009). This environment is typical of uranium mineralization in the Yilgarn Craton, Western Australia (e.g., Yeelirrie, Lake Way, Centipede, Thatcher Soak, and Lake Maitland deposits; Cameron, 1990; McKay and Miezitis, 2001; Lally and Bajwah, 2006; Fig. 1) and southern Africa, particularly Namibia (e.g., Langer-Heinrich and Trekkopje deposits, Central Namib Desert) (IAEA, 2009). Yeelirrie and Langer-Heinrich are the two largest calcrete-hosted deposits in the world, with ~56,000 tonnes and ~41,000 tonnes (UDEPO) of uranium respectively (IAEA, 2009). There is no significant calcrete-hosted uranium mineralization reported in China to date.

Calcrete-uranium deposits are broadly defined as young (Cenozoic), near-surface uranium concentrations within sediments and soils, although they also occur in peat bogs and karst terrains (McKay and Miezitis, 2001). A feature of these deposits is the dominance of carnotite [$K_2(UO_2)2(VO_4)_2{\cdot}3(H_2O)$] as the main uranium-bearing mineral. The carnotite is commonly a late-stage precipitate that coats or infills voids and cracks in the sediments, usually fine-grained surficial sand and clay cemented by secondary calcium and magnesium carbonates, along with gypsum, ferric oxides, manganese oxides and halite. Calcrete uranium deposits typically form under semi-arid to arid climatic conditions in regions where deeply-weathered, uranium-rich granites and mafic rocks coexist. Carnotite precipitates show evidence of dissolution and re-precipitation that reflect modification of chemical conditions following periodic influx of less-saline, alkaline groundwater (Bowell et al., 2009).

A typical model for the origin and formation of surficial calcreted-hosted uranium deposits is summarized in Fig. 15, based on common key features identified in Australian deposits (e.g., Yeelirrie and Lake Way). Deposits have also been classified into three main types, related to their geomorphological setting (Butt et al., 1984): valley (channels), playa (platforms), and terrace (deltas) deposits. The uranium sourced from uraniferous granites in the region is transported in mildly oxidizing saline alkaline groundwater solutions in constricted drainages to semi-closed basins with variable evaporative conditions. General characteristic of calcrete-hosted deposits, with reference to Bowell et al. (2009) and McGeough, pers comm. include:

1) significant areas of uranium-enriched bedrock, which are obvious in airborne radiometric imagery at both regional and continental scales, generally derived from Archean and Proterozoic weathered granites;
2) mostly late Cenozoic paleovalley systems drained these areas and discharged into lakes containing non-pedogenic carbonate deposits, as well as hosting channel calcrete formations, where uranium transport is by shallow groundwater drainage in areas of low topographic gradient;
3) a periodic wet and dry climatic region whereby there were long periods of wet developing drainage systems and dry allowing evaporation (e.g., Wiluna of WA and Napperby of NT);
4) carnotite mineralization in calcrete usually increases in the 'deltaic' segments of fluvial discharge into broader lake systems adjacent to paleovalleys;
5) almost all deposits show remarkably similar lithologies, i.e., deeply weathered zone of saprolitic clay overlying a granite basement, and/or alluvial clay overlying highly weathered basement with anomalous vanadium content;
6) uranium host materials formed in low-energy conditions dominated by calcrete and silcrete (e.g., approximately 25% of the carnotite mineralization of the Wiluna and Napperby deposits of Australia is hosted in calcrete/silcrete layers),

Table 4
Major calcrete uranium deposits and prospects in Australia (from Jaireth et al., 2015). Uranium resource data from OZMIN.

Deposits/prospects	State	Type	Ore (Mt)	Grade (%)	Uranium (t)
Anketell	WA	Valley	16.30	0.014	2308
Bellah Bore East	WA	Valley	0.35	0.018	62
Centipede	WA	Valley	12.94	0.043	5530
Dawson-Hinkler Well	WA	Valley	13.09	0.026	3463
Double 8 – Ponton	WA	Valley	26.00	0.025	6614
Hillview	WA	Valley	27.60	0.015	4072
Jailor Bore	WA	Unknown	1.43	0.050	716
Lake Maitland	WA	Playa	20.80	0.041	8564
Lake Mason	WA	Valley	9.10	0.016	1428
Lake Raeside	WA	Valley	6.80	0.025	1701
Lake Way	WA	Valley	9.95	0.045	4476
Lake Way South	WA	Playa	0.22	0.021	45.5
Lakeside (Lake Austin)	WA	Playa	0.62	0.042	265
Napperby	NT	Valley	9.34	0.030	2843
Nowthana	WA	Valley	11.90	0.047	8066
Peninsular Uranium	WA	Valley	9.75	0.014	1364
Thatcher Soak	WA	Valley	21.60	0.027	5916
Windimurra (U)	WA	Valley	19.00	0.015	2900
Wondinong	WA	Valley & Playa	6.50	0.016	1020
Yeelirrie	WA	Valley	50.05	0.111	55,599
Yuinmery	WA	Playa	1.581	0.031	496

fine sand/silt and clay (e.g., approximately 70% of the carnotite mineralization in these Australian deposits is hosted in silt and clay);

7) the carnotite mineralization is associated with secondary deposition of calcite, dolomite, gypsum, salt, celestine and barite, indicative of evaporative brine concentration;
8) as a common feature, the calcrete uranium mineralization is associated with highly saline water (1–3 times sea water salinity), even though the salinity of both upstream and downstream groundwaters is significantly lower;
9) carnotite mineralization occurs in fractures and vughs within a calcrete layer (often silicified or dolomitic) and as disseminated coatings on quartz grains in fine sands and on clay;
10) the mineralization depth is generally shallow, occurring mostly between the surface and ~15 m (at Yeelirrie, mineralization extends to 32 m below surface);
11) vanadium mainly sourced from greenstone and/or granite is necessary in forming carnotite mineralization (e.g., Wiluna, Napperby and Yeelirrie deposits), although its source of vanadium is not always obvious.

2.6.1. Calcrete-uranium in Australia

In Australia, most known calcrete-hosted uranium deposits and prospects are located in the Cenozoic paleovalleys incised in the Yilgarn Craton, Western Australia (Fig. 1; Table 4). Here, surficial uranium is deposited in valley-fill sediments along the trunklines of Cenozoic paleovalleys (e.g., Yeelirrie – the world's largest surficial deposit in the Yeelirrie Paleovalley, and Lake Way), and in playa lake sediments (e.g. Lake Maitland), as well as in calcrete terraces in dissected valleys (less common, mainly in the Gascoyne Province) (Mann and Deutscher, 1978; Cameron, 1990; McKay and Miezitis, 2001; Lally and Bajwah, 2006) (Figs. 1 and 15). These, and other significant calcrete uranium occurrences in the region, are confined largely to the northern Yilgarn Craton and overlie and are adjacent to weathered Archean granite and greenstone basement rocks, which provide a source of soluble uranium and vanadium necessary to form carnotite (Mann and Deutscher, 1978). The calcrete formed in the paleovalley sediments is relatively young (Mann and Horowitz, 1979) and reflects the change to more arid conditions, mostly post Miocene or Pliocene. The gradients of the paleodrainages in the mineralizing areas are generally low. For example, in the area of Yeelirrie deposit longitudinal gradients decrease from approximately 0.12% upstream to 0.06% near the ore body (Cameron, 1984), and in the area of the Lake Way deposit, the gradients range between 0.155% in the north and northeast to 0.06% near the lake (French and Allen, 1984).

Carbonate was precipitated from groundwater usually in the central and lower regions of the paleovalley where the watertable was close to the surface and evaporation and evapo-transpiration rates were sufficiently high to concentrate calcium and magnesium ions. According to Mann and Horowitz (1979), carbonate deposits formed initially within the zone of saturated sediments. Continued deposition and crystallization of carbonate caused mounding of older carbonate, which displaced overlying sediments and was pushed upwards above the watertable where the carbonate was recrystallized and hardened. Mineralization is generally concentrated near the groundwater table in sediments consisting of gypsiferous clays and muds. Uranium in groundwater, as uranyl carbonate complexes, combined with vanadium and potassium to precipitate carnotite in areas of valley calcretes, either through groundwater mixing or changed chemical conditions resulting in the solubility product of carnotite being exceeded (Gaskin et al., 1981).

3. Geological models

Although every known fluvial uranium deposit has its own distinctive characteristics, paleovalley-related uranium mineralization models have proven to have universal application. The key common factors of these models include uranium-rich source rocks, paleovalley networks, oxidizing groundwaters and a suitably porous and reduced sediment host, or chemical and environmental conditions that favor formation and precipitation of uranium minerals (e.g., uraninite, coffinite, carnotite) from oxidized fluids. Large areas of stable geological provinces and cratons satisfy these criteria. The successful combination of these factors is demonstrated by the numerous uranium deposits associated with paleovalleys of Australia and China. Most of the significant paleovalley-related uranium occurrences are in sediments of Mesozoic to Cenozoic age and this is in part due to the high organic content in the paleovalley sediments deposited at times of warm and wet climatic conditions with widespread colonization by land plants (e.g., Alley and Lindsay, 1995; Spirakis, 1996).

Similar to other places (e.g., USA, Kazakhstan and Namibia), paleovalley-related uranium deposits in Australia and China have the following characteristics:

1) Paleovalleys largely drained deeply weathered, high-uranium source rocks. In most cases, the primary uranium source can be identified in nearby uranium-rich basement rocks which have shed sediment into the basin.
2) Most such type uranium mineralization occur in Mesozoic and Cenozoic sediments; a likely result of changing paleoclimatic conditions during the Mesozoic and Cenozoic with associated weathering and erosion of granitic/metamorphic provenances and subsequent supply of oxygenated solutions under arid to semi-arid climatic regimes.
3) Host-rocks were deposited generally in paleovalley-related settings, including alluvial fan, channel, lagoon, estuarine in marginal basin.
4) Host-rock units are alluvial/fluviatile/lacustrine to marginal marine sandy sediments, particularly medium to coarse grained, sometimes interbedded with mudstone.
5) The host-rock units are those with good regional groundwater transmissivity. Porous sandy host-rocks are bounded by less permeable mudstone units, which is important for focusing oxidized U-bearing groundwaters into the sedimentary sequence with the development of redox fronts.
6) Host-rock calcretes/silts are generally buried by thin sediment cover.
7) Fossil carbonized plant matter or humic matter and reducing conditions in host rocks are commonly present.
8) Uranium concentrations are controlled by sedimentary and diagenetic-epigenetic features but may be related indirectly to tectonic structures and basement composition that potentially modify sedimentation, groundwater flow or groundwater composition.
9) Uranium is precipitated along a redox boundary [at the contacts between oxidized (altered) and reduced (non-altered) rocks] at the lateral margins of paleovalleys.
10) The mineralizing solutions were low-temperature groundwater.
11) Sedimentary and diagenetic uranium mineralization takes place generally in paleovalleys that incised low-relief cratonic regions with low-angle basinward discharge gradients which aids in deposit preservation. Periods of uplift are important in initiating erosion, the development of paleovalleys and gravity-driven flow of oxidizing ground waters. For instance, neotectonic activity is ongoing in some regions and

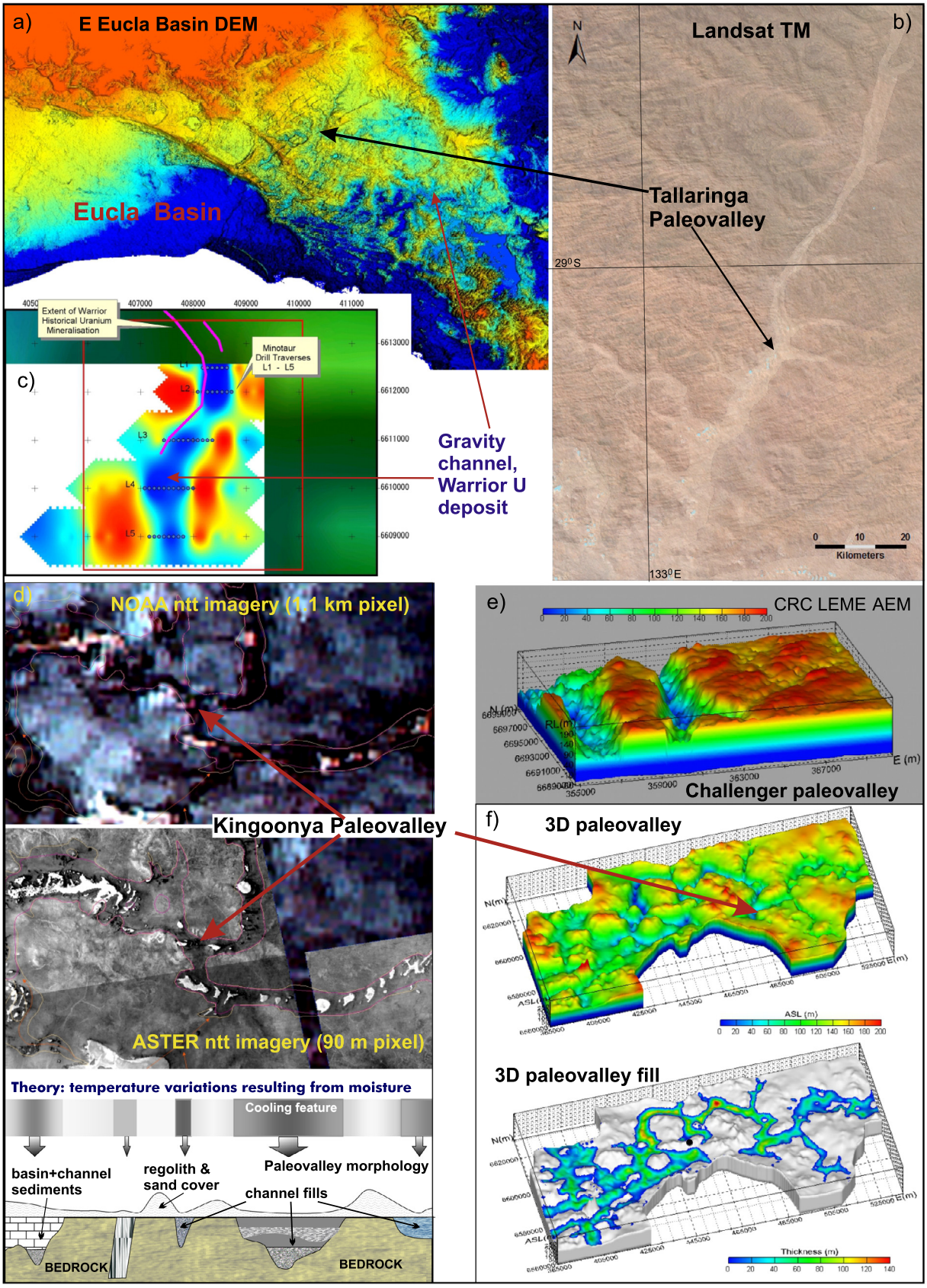

Fig. 16. Comparison of some methods in mapping paleovalleys: a) DEM imagery (for the location see Fig. 1a), b) Landsat 7 TM, c) gravity, d) NOAA NTT and ASTER NTT with Schematic night-time thermal (NTT) interpretation for a record of the stored heat being emitted from surface and subsurface features of paleovalleys and outcropping bedrock/basement (after Hou et al., 2017), e) Electromagnetic (AEM), and f) 3D modelling.

may be a significant factor in channeling fluids along faults and/or redistribution of uranium resulting in subsequent epigenetic deposits.

12) For calcrete uranium mineralization, it is important that Cenozoic paleovalley systems drain uranium-enriched bedrock with anomalous vanadium content.

The genetic models proposed for paleovalley-related uranium deposits worldwide are mostly consistent in that uranium concentrations in permeable sandstone were the result of low-temperature oxidized solutions, which leached uranium from the source rocks and precipitated uranium mineralization at a chemical interface usually involving a reducing agent (Dahlkamp, 1993). These models have been applied in Australia and China at local scale with some success and there is broad consensus that considerable scope exists for ongoing discovery of paleovalley-related uranium mineralization on a scale comparable to that discovered in Kazakhstan and USA. Variations to the models reflect local conditions and include the source of uranium, groundwater characteristics and transportation pathways, and type and distribution of reducing agents which affect precipitation of uranium minerals (Abzalov, 2012).

4. Exploration methodology

Hou et al. (2014) integrated and summarized the exploration methodology for paleovalley-related uranium deposits through the IGCP (514) Project. Exploration for such deposits has traditionally focused on defining paleovalleys and changes in a channel's course resulting in a reduction of channel flow, with consequent accumulation of organic matter (reducing material) and buildup of sandy sediments (e.g., point bar and overbank deposits). Other targets include channel confluences that provide an opportunity for mixing of fluids with different oxidation potential (Eh). Exploration techniques, often using conceptual geological modelling, have been developed to define channel morphology even where these are buried by over a hundred meters of exotic cover sediment (e.g., remote sensing, AEM; Hou and Mauger, 2005; Hou et al., 2001, 2003). Successful procedures can be developed for defining paleovalleys by combining imagery, geological, and geophysical data, with broader understanding of continental sedimentary processes and paleoclimatic history of a region to constrain architectural and evolutional models of channel development (Hou et al., 2001).

While paleovalleys have proven highly prospective for uranium, exploration can be problematic. One of the major difficulties associated with poorly-defined buried paleovalleys is undertaking exploration over large areas beneath substantial overburden without having to resort to costly, close-spaced drilling. Techniques that allow for precise geometric definition of paleovalleys and associated fluvial channels are therefore important in the overall effectiveness of exploration. Remote sensing, digital topography, geophysical and computer modelling techniques have proven to be useful and important tools in the delineation of paleovalleys (Hou, 2008; Hou and Mauger, 2005; Hou et al., 2001; 2003; 2007a). Knowledge and evidence from sedimentology is combined with other geological and geophysical characteristics to arrive at a general reconstruction of paleovalley architecture and history. Physical property contrasts that exist between the paleovalley sediments and the underlying bedrock can be differentiated by various geophysical methods to locate the incised-valley architecture (Hou et al., 2003). Where the physical property contrast between the paleovalley fills and the surrounding geology is poor (i.e., younger paleovalley incised into older basinal sediments, e.g., the Lake Frome region of South Australia), difficulties can arise in selecting effective methods to explore paleovalleys (Hou et al., 2007a), which are discussed below.

4.1. Paleovalley mapping

A regional-scale map of paleodrainage and Cenozoic coastal barriers of South Australia was released by Geological Survey of South Australia in 2007 (Hou et al., 2007a), and upgraded in a second edition (Hou et al., 2012), available in hardcopy and GIS. It is most useful example in the conceptual stage of exploration programs. The thematic map includes time-scaled paleovalleys, paleocoastal barriers and strandlines, together with known mineral occurrences, in particular uranium and heavy minerals. When used in combination with other spatial layers, in particular geology and geophysics, the 'essential ingredients' for a particular uranium mineralization model can be compared and evaluated in order to identify areas with potential to host uranium. In most cases, additional techniques will be required to define the detail of the paleovalleys at the local-scale, particularly in a target (tenement) area (Fig. 16).

4.1.1. Remote sensing imagery

While a *Digital Elevation Model (DEM)* may not directly show the distribution of paleovalley landforms, it can provide indirect associations related to links between modern and ancient (e.g., Mesozoic, Paleogene, Neogene) landscapes, because modern drainages usually erode relative soft zones and are often related to previous paleovalleys (Fig. 16a). With increasing resolution, the detail of interpretation will usually increase. However, the regional-scale interpretation of paleovalleys may be complicated by too much detailed information derived from high resolution DEMs. Processed *Landsat TM* satellite imagery is useful for regolith-landform mapping, particularly when draped over a DEM to enhance terrain visualization, which can be influenced by types of paleovalley sedimentation (e.g., channel silcrete accumulated along the Tallaringa paleodrainage system of South Australia; Fig. 16b). These maps can be used to identify paleovalleys where the paleochannel has an influence on surface features and regolith materials (e.g., vegetation association, arrangement of playa lakes, alluvial terraces, silicification). Compared to Landsat imagery (7 bands), *ASTER* and *Hyperspectral Remote Sensing* contain more spectral bands (14 and >100 bands respectively) which can potentially distinguish most surficial features related to paleovalley sediments. The detector and orbital configuration of *NOAA–AVHRR* and *ASTER* night-time satellites provide thermal data that are potentially useful for detecting temperature variations in subsurface sediments related to the elevated moisture content of the channel (Fig. 16c). Thermal data can therefore be used as a quick and inexpensive method for mapping paleovalley sediments, particularly when used in conjunction with other (e.g., geophysical) data sets and preferably with some drill hole or geological control.

4.1.2. Geophysical methods

Paleovalley *magnetic* (either positive or negative) anomalies may be defined if high resolution surveys are used and if there are sufficient magnetic minerals in the channels or measurable magnetic contrast between the channel sediments and bedrock. Mesozoic and/or Cenozoic paleovalleys are not usually visible on regional magnetic data, as they are relatively shallow features, but careful use of detailed survey data may assist in locating channel deposits (e.g., basalt flows buried within the paleovalley generally showing a positive magnetic anomaly). *Gravity* anomalies in the Earth's gravitational field can in some cases be used to define the thickness and extent of the fluvial sediments, and hence paleovalleys (Fig. 16d), due to the contrast in density between the sediments (e.g., sand and clay having a density of around 1.8 g/cc;

Berkman, 1995) and fresh bedrock (e.g., granitic basement having a density of 2.7 g/cc; Berkman, 1995). *Radiometric* data is not a mapping tool for buried paleovalleys, but is effective in linking physical dispersion of sediment with uranium-rich source regions, especially when overlain on DEM, Landsat, NOAA, or AEM images. Surficial uranium deposits associated with calcrete in paleodrainage sediments have been successfully delineated using airborne radiometrics, due to localized, high uranium counts (e.g., Wilford et al., 2009). *Electromagnetic* (AEM and TEM) methods measure the electrical conductivity of the ground both laterally and vertically. The data can be processed to show ground conductivity as a function of depth and can thus define channel sediments due to their porosity, moisture content and the conductivity of the groundwater within them. This technique has been used successfully in South Australia for paleovalley identification, e.g., Garford paleovalley and Kingoonya Paleovalley (Fig. 16e). The technique however, is problematic for application in places where channel sediment fill is incised into basinal sediments because of similar conductive features between channel and basin sediments, such as the northwest Callabonna Sub-basin, South Australia. Regional AEM data over the Callabonna Sub-basin, however, have been effective in mapping fault displacement of paleovalley sediments and in identifying areas where groundwaters of differing salinities interact, both of which appear to be significant local factors influencing uranium deposition (Michaelsen et al., 2012). Shallow *seismic* reflection and refraction imaging can be used for investigating subsurface structure (particularly in sedimentary terrains) and therefore have application for delineating paleovalleys. By integrating reflection and refraction techniques, it is possible to determine paleovalley depths, variability of materials, and the morphologies of both shallow and deeper strata (Drummond, 2002). The *Ground penetrating radar (GPR)* method is useful for delineating the geometry, structure and thickness of channel deposits by providing a high-resolution image of subsurface features in the form of a cross-section view. However, this technique is only suitable for shallow investigation (up to tens of meters in ideal conditions).

4.1.3. Structural and basement geology

Basement structure and lithology may be important in controlling channel morphology, and ultimately the location of uranium mineralization. Holbrook and Schumm (1999) showed that an increase in slope along the course of a channel, commonly related to uplift, would result in increased sinuosity. The Honeymoon uranium deposit of South Australia is located at a pronounced bend in the host Yarramba paleovalley, where gravity and magnetic imagery indicate a fault cross-cutting the channel (Southern Cross Resources Australia Pty Ltd., 2000). Here, the channel has more deeply incised the underlying basement rocks at a point which corresponds to a regional-scale redox interface within the basement lithologies.

4.1.4. Sedimentological analysis

Sedimentological data and interpretation, when combined with other geological and geophysical information can be used to provide a general reconstruction of the paleovalley architecture and history (Hou and Mauger, 2005). Knowledge of the stratigraphic and geographic evolution of the area is necessary to interpret the regional depositional, environmental and paleogeographic framework (Hou, 2008). Sequence stratigraphic methods, supplemented by studies in paleoclimate, mineralogy, petrology and geochemistry of the sediments have proved useful in studies on the Gawler Craton of South Australia (Hou et al., 2001; 2003).

4.1.5. 3D modelling

Where sufficient data are available, 3D visualization models of the paleovalley landform can provide crucial insights into the landscape evolution and controls on the dynamics of paleorivers. The paleovalleys interpreted from GIS and geophysical datasets can be viewed either as 3D plume diagrams, mapped onto surfaces, or as slices, such as the paleovalley and paleolandscape with exploded layers separating variously aged paleosurfaces (Fig. 19f; Hou, 2008; Hou et al., 2004).

4.2. Location, definition and assessment of mineralization

While groundwater geochemistry for uranium in solution usually gives misleading results, multi-element data from a limited number of boreholes can be used to distinguish prospective sediments by taking into account pH, equilibrium with carbonate minerals, and carbonaceous matter content (Giblin, 1987). The delineation of paleovalley-related uranium by surface geochemical methods is not well established over known uranium districts in Australia or China, particularly for deeply buried deposits. No successful methods have been reported to date. Elsewhere, techniques that have been used with some success include gas methods (GVP, radon), soil sampling (shallow deposits) and CHIM (electrogeochemical) methods (Fabris et al., 2006; Luo et al., 2004, 2006).

When paleovalleys are delineated, *Test drilling* is required to check and refine the paleovalley interpretation (Hou, 2008; Hou et al., 2003). Drillhole data need to be continually updated to refine and improve the detail of paleovalley mapping. Drilling in paleovalleys with relatively unconsolidated sediments mainly include mud rotary and RC percussion with air core, or sonic drilling to recover core. Gamma and Prompt Fission Neutron (PFN) logging are widely used to estimate the grade of *in situ* uranium mineralization and the state of radioactive disequilibrium, with chemical analysis used on relatively few samples, primarily to confirm uranium grade in probable ore zones and to establish calibration for PFN and gamma logging (Penney, 2012). Down-hole geophysical logs in combination with visual logging of drill samples, provide the main inputs for sedimentary facies analysis and reconstruction of paleovalley architecture to model the uranium distribution and sedimentological constraints on mineralization. All of these aim at improving the understanding of facies and micro-environment, potential paleo-redox fronts and mineralization processes occurring within paleovalley systems. These data are used to develop predictive models of paleovalley-related uranium systems with the intention of reducing exploration costs.

5. Discussion and conclusions

5.1. Reductants

The amount of reductant required to form a sandstone-hosted uranium deposit is a point of current debate, with some studies identifying the quantity or quality of reductants in the host sediment as insufficient or unsuitable to form the deposit (e.g., Beverley deposit in the Namba Formation; Michaelsen et al., 2012; 2016). The organic content of the sandstone aquifer in the Chu-Sarysu Basin of Kazakhstan, which hosts several world-class sandstone-hosted uranium deposits, is substantially lower (generally b 0.03 to 0.05 wt.%) than that of uranium-hosting sandstone units in the Wyoming Basin of USA (0.5 wt.%; Jaireth et al., 2008). The low organic carbon content of the aquifers in the Chu-Sarysu Basin may have allowed oxidized groundwaters to flow to considerable distance (~350 km between redox fronts and probable source rocks), allowing for the build-up of a high concentration of dissolved uranium (Jaireth et al., 2015). Minor content of reductants is probably sufficient to form smaller uranium deposits, with evidence of the extent of reductant largely eliminated by the processes resulting in formation of the deposit (McGeough, pers

comm.). Larger uranium deposits may develop from the influx of mobile reductants (hydrocarbons and associated gases) from hydrocarbon source rocks at greater depths in basins hosting sandstone uranium deposits (Jaireth et al., 2008; Li et al., 2008; Pechenkin, 2014). The influx of mobile gaseous reductants from organic matter may also modify the activity of anaerobic bacteria in sandstone aquifers leading to enhanced precipitation of uranium from oxidized groundwaters (Li et al., 2008; Jaireth et al., 2015; Michaelsen et al., 2016).

5.2. Source of uranium

The necessity for a proximal basement source of uranium to form a sandstone hosted or paleovalley-related deposit is another point of current debate, with some studies indicating that enrichment of uranium from leaching of uraniferous sands within the sedimentary environment is sufficient (e.g., Erlian, Ordos and Songliao basins of north China). Nevertheless, the presence of spatially related uranium-rich granites (such as the Mesoproterozoic Hiltaba Suite and broad equivalents in South Australia, and Archean granitoids in the Yilgarn Craton, Western Australia) is a desirable component of the mineral system. A spatial relationship is evident between areas of high uranium in basement and uranium mineralization within the surrounding sediments, e.g. Beverley and Four Mile deposits in close proximity to uranium-enriched granites and gneisses of the Mount Painter Inlier in the northern Curnamona Province. Paleovalleys on the Gawler and Yilgarn Cratons, incised during late Mesozoic and early Cenozoic times, also contain sediments sourced from uraniferous basement rocks, and these paleodrainage networks also host significant uranium occurrences.

5.3. Implications for sandstone-hosted or lignite-hosted deposits

As evidenced in the Mulga Rock and Nuheting uranium deposits as well as elsewhere in the Erlian Basin (e.g., Subeng and Naomugen deposits, Dahlkamp, 2009; sandstones of the Saihan Formation, Bonnetti et al., 2015b), significant synsedimentary uranium concentration and diagenetic mineralization are hosted in the mudstone/lignite layers. This means that a pre-existing stock of uranium was significantly present in the basin, particularly in the reduced muddy or lignitic layers, prior to the formation of roll front deposits. During the late diagenetic and epigenetic stages, part of the early stage mineralization was most likely remobilized despite the permeability of the host-rock being very low (Bonnetti et al., 2015a). If similar synsedimentary to diagenetic uranium mineralization occurs more widely in the basin within overbank deposits or directly within permeable channel sandstone layers of braided river system (e.g., sandy channel fills in the area of the Mulga Rock deposits, Hou et al., 2014; and sandstones of the Saihan Formation, Erlian Basin; Bonnetti et al., 2015b), therefore, it would potentially represent a major source of uranium for subsequent formation of roll front deposits in a basin (as for the Mulga Rock deposits in the Eucla Basin, Hou et al., 2014; and Bayinwula deposit in the Erlian Basin; Bonnetti et al., 2015b).

The comparison of the Mulga Rock and Nuheting deposits with other tabular sandstone-hosted deposits, such as Beverley, indicates a significant difference: i.e., the major primary uranium source of the latter (e.g., the Mt Painter Inlier in the Lake Frome region) was not the primary source of detritus at the time of sedimentation (Wülser, 2011). In contrast to the Mulga Rock and Nuheting deposits, therefore, very limited uranium was available in host units within the basin during initial syngenetic/diagenetic processes, although traps such as S-reducers-bearing aquifers and organic matter-rich facies were present (Bonnetti et al., 2015a). In the Ordos Basin and Callabonna Sub-basin, the uranium mineralization occurred when U-bearing groundwater infiltrated the sediments following tectonic uplift of the uranium-rich basement. In the case of the Callabonna Sub-basin, subsequent erosion of the uplifted basement rocks resulted in thick colluvial and fluvial younger deposits (Willawortina Formation) with dispersed uranium, that represents a potential large source of dispersed uranium available to be remobilized and concentrated, given suitable conditions. Awareness of the available uranium sources, reservoirs and concentration processes is the basis for developing geological models and concepts that will assist with planning exploration for discovery of further deposits.

6. Conclusions

Paleovalley-related uranium systems in Australia and China have four essential ingredients: 1) source rocks (i.e., leachable uranium, vanadium and potassium) linked to paleovalley systems, 2) paleovalleys/basin margins (i.e., transport pathway and site of accumulation), 3) physical and chemical environments for mineralization (e.g., paleo-geomorphology, groundwater flux and salinity, pH, Eh, climatic conditions) and, 4) pre- and post-mineralization settings for preservation (e.g., muddy layers, faulting, erosion). The presence of these key ingredients for uranium deposit formation make northern China and southern, western and northern parts of Australia highly prospective for paleovalley-related uranium deposits, in particular, sandstone-related styles but also surficial deposits.

Paleovalley-related uranium deposits of Australia and China occur in sedimentary marginal basins and their peripheral paleovalleys ranging in age from Carboniferous to Cenozoic, and are well represented throughout western, southern and northern Australia and northern China. Given the spatial proximity to the known source rocks, potential exists for the discovery of additional paleovalley-related uranium deposits in these regions. In the northern Curnamona Province of South Australia, for example, the highly uraniferous rocks of the Mount Painter and Mount Babbage Inliers provide a source for paleovalley-related deposits such as Beverley, Four Mile, and Pepegoona to the east of the inliers. Similar sedimentary sequences that flank the inliers to the north and west have potential for paleovalley-related deposits and are a focus of ongoing uranium exploration activity. Recent work by Skirrow (2009) and Hore and Hill (2009) highlight the potential also for sediments of Mesozoic age to also host uranium mineralization in these regions of South Australia.

Paleovalley-related uranium models are important for exploration as they can be used to integrate a wide variety of potentially significant geological factors leading to the formation of deposits. Improved understanding of geological controls and landscape history can assist with target definition and choice of technique when mapping paleovalley distribution. Regional exploration for paleovalley-related uranium deposits can be based initially on empirical data gained from known deposits. Models will evolve as additional data are gathered during exploration and from ongoing sedimentological studies. Exploration should begin with the delineation of paleodrainage by the examination of a combination of inexpensive surface and remotely sensed data and compared in GIS. The model can then be progressed using geophysical techniques and drilling. The ultimate aim is to construct 3D geological representations in which the sedimentary facies and depositional patterns can be mapped; alteration and facies trends traced; structural features identified; and finally the mineralizing system outlined and evaluated.

Mesozoic and Cenozoic organic-rich sand, clay, calcrete and lignite are hosts for sandstone, calcrete and lignite uranium deposits in the regions where paleovalleys have developed. These areas are a focus for ongoing and successful uranium exploration in both

Australia and China. Australia and China remain highly prospective for the discovery of new paleovalley-related uranium deposits, with night-time thermal imagery from remotely sensed data and local airborne geophysical surveys amongst the techniques now used to assist with defining paleovalley networks that drained uranium rich source rocks. Geological settings similar to that of the Chu-Sarysu and Syrdarya Basins of southern Kazakstan and Songliao and Ordos Basins of north China are present in hydrocarbon-bearing basins in Australia, including the hydrocarbon or H_2S-rich Cooper Basin below extensive organic-poor sandstone aquifers in the Eromanga Basin. Greater understanding of the factors influencing the effective reduction of uranium by hydrocarbons in shallow sandstone aquifers will invariably provide new exploration targets in these settings.

Acknowledgements

The concept for this paper was encouraged through the exchange of information resulting from collaborations between Geological Survey of South Australia, CNNC BRIUG and Saskatchewan Geological Survey. This review paper has benefited from various discussions with industry (e.g., Toro Energy Ltd, Heathgate Resources Pty Ltd, Red Metal Limited, Coffey Mining, Southern Cross) and with international researchers (e.g., from USA, Canada, Russia, Kazakhstan, India, and China) through IGCP-514. We are also grateful for the advice and discussions of Australian and Chinese geoscientists, especially Adrian Fabris, Bernd Michaelsen, Roger Fidler, Mark McGeough, Steve Hore, Tania Wilson, Alan Mauger, Laszlo Katona, Subhash Jaireth, Ian Roach, David Gray, Jindai Zhang, and Xianrong Luo on various aspects of uranium geology and geochemistry and the application of remote sensing, geochemical, geophysical and GIS techniques. The authors are gratefully acknowledge the comments of the reviewers, which led to improvement to the manuscript. The paper is published with the permission of Department of Premier and Cabinet South Australia and China National Nuclear Corporation (CNNC).

References

Abzalov, M.Z., 2012. Sandstone-hosted uranium deposits amenable for exploitation by in situ leaching technologies – a review. Trans. Inst. Min. Metall. Sect. B, Appl. Earth Sci. 121 (2), 55–64.
Adelaide Resources, 2009. Quarterly report period ending 31 December 2009. Adelaide Resources Ltd.
Adams, S.S., Curtis, H.S., Hafen, P.L., Salek-Nejad, H., 1978. Interpretation of postdepositional processes related to the formation and destruction of the Jackpile-Paguate uranium deposit, Northwest New Mexico. Econ. Geol. Bull. Soc. Econ. Geol. 73, 1635–1654.
Adams, S.S., Smith, R.B., 1981. Geology and recognition criteria for sandstone uranium deposits in mixed fluvial-shallow marine sedimentary sequences, south Texas: Final report, US-DOE, GJBX-4(81), pp. 145.
Alley, N.F., 1998. Cainozoic stratigraphy, palaeoenvironments and geological evolution of the Lake Eyre Basin. Palaeogeogr. Palaeoclimatol. Palaeoecol. 144, 239–263.
Alley, N.F., Lindsay, J.M., 1995. Tertiary. In: Drexel, J.F., Preiss, W.V. (Eds.), The Geology of South Australia, The Phanerozoic: Geological Survey of South Australia, Bulletin, 54(2), pp. 150–217.
Alley, N.F., Frakes, L.A., 2003. First known Cretaceous glaciation: Livingston Tillite Member of the Cadna-owie Formation, South Australia. Aust. J. Earth Sci. 50, 139–144.
Alley, N.F., Clarke, J.D.A., Macphail, M., Truswell, E.M., 1999. Sedimentary infillings and development of major Tertiary palaeodrainage systems of southcentral Australia. In: Thiry, M., Coincon, R.S. (Eds.), Palaeoweathering, palaeosurfaces and related continental deposits. International Association of Sedimentologists, pp. 337–366. Special Publications 27.
Aubakirov, K.B., 1998. On the deep origin of ore-forming solutions in the uranium deposits in platform sequence of depressions (with Chu-Sarysu Province as an example). Geol. Kazakhstan 2 (354), 40–47.
Bastrakov, E.N., Jaireth, S., Mernagh, T.P., 2010. Solubility of uranium in hydrothermal fluids at 25°–300°: implications for the formation of uranium deposits: Geoscience Australia, Record 2010/29. Geoscience Australia, p. 86.
Benbow, M.C., Lindsay, J.M., Alley, N.F., 1995. Eucla Basin and palaeodrainage. In: Drexel, J.F., Preiss, W.V. (Eds.), The Geology of South Australia, The Phanerozoic. Geological Survey of South Australia, pp. 178–186. Bulletin, 54(2).
Berkman, D.A., 1995. Gravity survey methods and tables. In: Berkman, D.A. (Ed.), Field Geologists Manual. 3rd edn. Australasian Institute of Mining and Metallurgy. Monograph 9, pp. 324.
Binks, P.J., Hooper, G.J., 1984. Uranium in Tertiary palaeochannels 'West Coast area', South Australia. Australasian Institute of Mining and Metallurgy. Proceedings 289, 271–275.
Bluck, R., 2009a. Inferred resource for the Blackbush Prospect western mineralised zone, Mullaquana Project. Uranium SA Ltd.. ASX Release, 4 May 2009.
Bluck, R., 2009b. Increased grade and thickness at the Mullaquana uranium project, progress results from infill drilling. Uranium SA Ltd.. ASX Release, 21 December 2009.
Bonnetti, C., Cuney, M., Malartre, F., Michels, R., Bourlange, S., Liu, X., 2014. Genesis of roll front-type uranium deposits in the Erlian Basin, NE China: The Bayinwula deposit. AusIMM Uranium Conference, 10–11 June, Perth.
Bonnetti, C., Cuney, M., Malartre, F., Michels, R., Liu, X., Peng, Y., 2015. The Nuheting deposit, Erlian Basin, NE China: synsedimentary to diagenetic uranium mineralization. Ore Geol. Rev. 69, 118–139.
Bonnetti, C., Cuney, M., Michels, R., Truche, L., Malartre, F., Liu, X., Yang, J., 2015. The multiple roles of sulfate-reducing bacteria and Fe-Ti oxides in the genesis of Bayinwula roll front-type uranium deposit, Erlian Basin, NE China. Econ. Geol. 110, 1059–1081.
Borshoff, J., Faris, I., 1990. Angela and Pamela uranium deposits. In: Hughes, F.E. (Ed.), Geology of the Mineral Deposits of Australia and Papua New Guinea. Australasian Institute of Mining and Metallurgy, Melbourne, pp. 1139–1142.
Bowell, R.J., Barnes, A., Grogan, J., Dey, M., 2009. Geochemical controls on uranium precipitation in calcrete palaeochannel deposits of Namibia, in Lentz, D.R., Thorne, K.G., Beal, K. (Eds), 24th International Applied Geochemistry Symposium, Fredericton, New Brunswick, Canada, Proceedings, 1: 425–430.
Boyle, D.R., 1982. The formation of basal-type uranium deposits in south central British Columbia. Econ. Geol. 77, 1176–1209.
Boyle, D.R., 1984. The genesis of surficial uranium deposits. Surficial Uranium Deposits IAEA TECDOC-322. IAEA, Vienna, pp. 45–52.
Brugger, J., Long, N., McPhail, D.C., Plimer, I., 2005. An active amagmatic hydrothermal system: The Paralana hot springs, northern Flinders Ranges, South Australia. Chem. Geol. 222, 35–64.
Brunt, D.A., 1990. Miscellaneous uranium deposits in Western Australia. In: Hughes, F.E. (Ed.), Geology of the mineral deposits of Australia and Papua New Guinea, Parkville, Victoria. Australasian Institute of Mining and Metallurgy, pp. 1615–1620. Monograph 14.
Bush, P.D., 2000. Development considerations for the Honeymoon ISL uranium project. Canadian Institute of Mining and Metallurgy. Bulletin 93, (1045), pp. 65–73.
Butt, C.R.M., Mann, A.W., Horwitz, R.C., 1984. Regional setting, distribution and genesis of surficial uranium deposits in calcretes and associates sediments in Western Australia. Surficial Uranium Deposits, IAEA TECDOC-322. IAEA, Vienna, pp. 121-127.
Cai, C.F., Li, H.T., Luo, X.R., 2005. Petroleum related origin for sandstone-hosted uranium deposits in the Dongsheng area, Ordos Basin (China). In: Mao, J.W., Bjerlein, F.P. (Eds.), Mineral Deposit Meeting the Global Challenge-Proceedings of the 8th Biennial Society for Geology Applied to Mineral Deposits Meeting. Springer Verlag, Berlin, pp. 229–302.
Cai, C., Dong, H., Li, H., Xiao, X., Ou, G., Zhang, C., 2007a. Mineralogical and geochemical evidence for coupled bacterial uranium mineralization and hydrocarbon oxidation in the Shashagetai deposit, NW China. Chem. Geol. 236, 167–179.
Cai, C., Li, H., Qin, M., Luo, X., Wang, F., Ou, G., 2007b. Biogenic and petroleum-related ore-forming processes in Dongsheng uranium deposit, NW China. Ore Geol. Rev. 32, 262–274.
Callen, R.A., 1990. CURNAMONA, South Australia, sheet SH54-14: Geological Survey of South Australia, 1:250 000 Series Map, Explanatory Notes.
Cameron, E., 1984. The Yeelirrie calcrete uranium deposit, Western Australia. IAEA TECDOC-322. IAEA, Vienna, pp. 157–164.
Cameron, E., 1990. Yeelirrie uranium deposit. In: Hughes, F.E. (Ed.), Geology of the Mineral Deposits of Australia and Papua New Guinea. Australasian Institute of Mining and Metallurgy, Melbourne, Victoria, Australia, pp. 1625–1629.
Callen, R.A., Alley, N.F., Greenwood, D.R., 1995. Lake Eyre Basin. In: Drexel, J.F., Preiss, W.V. (Eds.), The Geology of South Australia, The Phanerozoic, Vol. 2. Geological Survey of South Australia, pp. 188–194. Bulletin 54(2).
Chen, Z.B., Zhao, F.M., Xiang, W.D., Chen, Y.H., 2000. Uranium province in China. Acta Geol. Sinica 74, 587–594.
Clarke, J.D.A., 1993. Stratigraphy of the Lefroy and Cowan paleodrainages, Western Australia. R. Soc. Western Aust., J. 76, 12–23.
Clarke, J.D.A., Gammon, P.R., Hou, B., Gallagher, S.J., 2003. Middle to Upper Eocene stratigraphic nomenclature and deposition in the Eucla basin. Aust. J. Earth Sci. 50, 231–248.
Conor, C.H.H., 2004. Geology of the Olary Domain, Curnamona Province, South Australia. Department of Primary Industries and Resources, South Australia. Report Book 2004/8.
Cross, A.J., Jaireth. S., Hore, S.B., Michaelsen, B.H., Schofield, A., 2010. SHRIMP U-Pb detrital zircon results, Lake Frome region, South Australia, Geoscience Australia Record 2010/46, Geoscience Australia, Canberra
Cuney, M., 2010. Evolution of uranium fractionation processes through time; driving the secular variation of uranium deposit types. Econ. Geol. Bull. Soc. Econ. Geol. 105, 553–569.
Cuney, M., Kyser, K., 2008. Recent and not-so-recent developments in uranium deposits and implications for exploration, 39. Min. Assoc. Can.. 257 pp.

Curtis, J.L., Brunt, D.A., Binks, P.J., 1990. Tertiary palaeochannel uranium deposits of South Australia. In: Hughes, F.E. (Ed.), Geology of the mineral deposits of Australia and Papua New Guinea. Australasian Institute of Mining and Metallurgy, pp. 1631–1636. Monograph 14.
Curnamona Energy, 2009. Annual Report 2009. Curnamona Energy Ltd.
Dahlkamp, F.J., 1993. Uranium Ore Deposits. Springer-Verlag, Berlin Heidelberg.
Dahlkamp, F.J., 2009. Uranium Deposits of the World. Springer Ed., Asia. 493 pp.
Dai, J., 1996. Metallogenic geological conditions of the Russian paleovalley uranium deposits. Uranium Geol. 12 (6), 336–340 (in Chinese with English abstract).
de Broekert, P.P., 2002. Origin of Tertiary inset-valleys and their fills, Kalgoorlie, Western Australia Unpublished Ph.D. thesis. Australian National University, Canberra, Australia. 388 p.
DeVoto, R.H., 1978a. Uranium geology and exploration: lecture notes and references. Colorado School Mines, Golden. 396p.
DeVoto, R.H., 1978b. Uranium in Phanerozoic sandstone and volcanic rocks. In: Kimberley, M.M. (Ed.), Uranium deposits, their mineralogy and origin, 3. Mineralogical Association of Canada, pp. 293–306. Short Course Handbook.
Dickson, B.L., 1984. Uranium series disequilibrium in the carnotite deposits of Western Australia. Surficial Uranium Deposits TECDOC-322. IAEA, Vienna, pp. 165-170.
Dong, W.M., Lin, J.R., Xia, Yu, L., Qi, D.E., 2005. Alteration characteristics of the sandstone-type uranium deposit in Qianjiadian, Inner Mongolia, in: Mao, J., Bierlein, F. (Eds.), Mineral Deposit Research: Meeting the Global Challenge. Proceedings of the Eighth Biennial SGA Meeting Beijing, China, 18–21 August 2005, pp. 249–251.
Dou, L., Chang, L., 2003. Fault linkage patterns and their control on the formation of the petroleum systems of the Erlian Basin, Eastern China. Mar. Petrol. Geol. 20, 1213–1224.
Dou, L., Zhu, Y., Yang, T., Xu, S., Ping, X., 1998. Origins of heavy oils in the Erlian Basin, NE China. Mar. Petrol. Geol. 15, 658–670.
Douglas, G.B., Butt, C.R.M., Gray, D.J., 2003. Mulga Rock Uranium and Multi-Element Deposits. Officer Basin, WA, CRC LEME, CSIRO Exploration and Mining, Bentley, Bentley.
Douglas, G.B., Butt, C.R.M., Gray, D.J., 2011. Geology, geochemistry and mineralogy of the lignite-hosted Ambassador palaeochannel uranium and multi-element deposit, Gunbarrel Basin, Western Australia. Mineral. Deposita 46, 761–787.
Drummond, B., 2002. Seismic surveys for imaging the regolith, in Papp, É., (Ed.), Geophysical and remote sensing methods for regolith exploration, CRCLEME Open File Report 144, pp. 95–99.
Edgoose, C.J., 2013a. Amadeus Basin. In: Ahmad, M., Munson, T.J. (Eds.), Geology and mineral resources of the Northern Territory. Northern Territory Geological Survey, Darwin, pp. 23:21–23:70.
Edgoose, C.J., 2013b. Ngalia Basin. In: Ahmad, M., Munson, T.J. (Eds.), Geology and mineral resources of the Northern Territory. Northern Territory Geological Survey, Darwin, pp. 24:21–24:24.
Elburg, M.A., Bons, P.D., Dougherty-Page, J., 2001. Age and metasomatic alteration of the Mt Neill Granite at Nooldoonooldoona Waterhole, Mt Painter Inlier, South Australia. Aust. J. Earth Sci. 48, 721–730.
Energy and Minerals Australia, 2010. Development and exploration activities report, three months to 30 September 2010.
Fabris, A.J., Conor, C.H.H., Crooks, A.F., Burtt, A.C., 2004. (Compilers). Uranium prospects of the southern Curnamona Province and cover sequences, South Australia. South Australia. Department of Primary Industries and Resources. Report Book 2004/22.
Fabris, A.J., Keeling, J.L., Fidler, R., Hou, B., Luo, X., Zeng, N., 2006. Chinese CHIM electrogeochemical method: Field trials 2005, South Australia: South Australia. Department of Primary Industries and Resources. Report Book 2006/23.
Fan, X., Nie, F., Chen, Y., Wang, W., 2008. Discussion on age and paleo geographical environment of ore bearing strata for sandstone-type uranium deposits in Bayanwula area, Erlian Basin. Uranium Geol. 24–3, 151–154 (in Chinese with English abstract).
Feng, Z., Nie, F., Yan, Z., Jiang, L., Gu, S., Chen, L., 2014. Structure and fluid evolution of the western slope of Songliao Basin and its relation to sandstone type uranium mineralization. J. East China Inst. Technol. (Nat. Sci.) 37 (1), 13–20 (in Chinese with English abstract).
Fidler, R.W., Pope, G.J., Ivanac, J.F., 1990. Bigrlyi uranium deposit. In: Hughes, F.E. (Ed.), Geology of the Mineral Deposits of Australia and Papua New Guinea. Australasian Institute of Mining and Metallurgy, Melbourne, pp. 1135–1138.
Finch, W.I., Davis, J.F., 1985. TI: Sandstone-type uranium deposits; an introduction. In: Finch, W.I., Davis, J.F. (Eds.), Geological environments of sandstone-type uranium deposits, pp. 11–19.
Fischer, R.P., 1970. Similarities, differences, and some genetic problems of the Wyoming and Colorado Plateau types of uranium deposits in sandstone. Econ. Geol. 65, 778–784.
Fraser, G.L., Neumann, N.L., 2010. New SHRIMP U-Pb zircon ages from the Gawler Craton and Curnamona Province, South Australia, 2008–2010. Geoscience Australia Record 2010/16.
French, R.R., Allen, J.H., 1984. Lake Way uranium deposit, Wiluna, Western Australia. Surficial Uranium Deposits, TECDOC-322. IAEA, Vienna, pp. 149–157.
Fricke, C., 2008. Definitions of Mesoproterozoic igneous rocks of the Curnamona Province. the Ninnerie Supersuite: South Australia. Department of Primary Industries and Resources. Report Book 2008/4.
Fricke, C., Reid, A., 2009. Alteration of uranium-rich granite and its relationship to uranium mineralisation in the Honeymoon Area, South Australia. Department of Primary Industries and Resources, South Australia. Report Book 2009/4.
Fulwood, K.E., Barwick, R.E., 1990. Mulga Rock uranium deposits, Officer Basin. In: Hughes, F.E. (Ed.), Geology of the Mineral Deposits of Australia and Papua New Guinea. Australasian Institute of Mining and Metallurgy, Melbourne, pp. 1621–1623.
Fyodorov, G.V., 2001a. Uranium deposits of the Inkay - Mynkuduk ore field, Kazakhstan. IAEA TECDOC-1425, pp. 95–112.
Fyodorov, G.V., 2001b. Industrial types of uranium deposits in Kazakhstan. IAEA TECDOC-1258, pp. 77–83.
Gaskin, A.J., Butt, C.R.M., Deutscher, R.L., Horwitz, R.C., Mann, A.W., 1981. Hydrology of uranium deposits in calcretes of Western Australia: Energy Resources of the Pacific Region. Australian Association of Petroleum Geologists. special volume A177, pp. 311–316.
Giblin, A., 1987. Applications of groundwater geochemistry to genetic theories and exploration methods for Early Tertiary sediment-hosted uranium deposits in Australia. Uranium 3, 165–186.
Giralia Resources, 2007. Annual report 2007. Giralia Resources NL.
Grutt, E.W., 1971. Prospecting criteria for sandstone-type uranium deposits. In: Bowie, S.H.U. (Ed.), Uranium prospecting handbook, Proceedings of the NATO-sponsored Advanced Study Institute on Methods of prospecting for uranium minerals. The Institute of Mining and Metallurgy, London, pp. 47–78.
Goldhaber, M.B., Reynolds, R.L., Rye, R.O., 1978. Origin of a South Texas roll-type deposit; II, Sulfide petrology and sulfur isotope studies. Econ. Geol. Bull. Soc. Econ. Geol. 73, 1690–1705.
Goldhaber, M.B., Reynolds, R.L., Rye, R., 1983. Role of fluid mixing and fault-related sulfide in the origin of the Ray Point uranium district, South Texas. Econ. Geol. 78, 1043–1063.
Heathgate Resources, 1998. Beverley uranium mine, environmental impact statement. Heathgate Resources Pty. Ltd., ISBN 0646357158.
Heathgate Resources, 2007. Mining Proposal for proposed extension of Beverley Mine. Heathgate Resources Pty Ltd.
Heathgate Resources, 2008. Beverley Four Mile project public environment report and mining lease proposal. Heathgate Resources Pty Ltd.
Holbrook, J., Schumm, S.A., 1999. Geomorphic and sedimentary responses of rivers to tectonic deformation: a brief review and critique of a tool for recognizing subtle epeirogenic deformation in modern and ancient settings. Tectonophysics 305, 287–306.
Holland, H.D., 2006. The oxygenation of the atmosphere and oceans. Philos. Trans. R. Soc. Lond. B Biol. Sci. 361, 903–915.
Hore, S.B., Hill, S.M., 2009. Palaeoredox fronts: setting and associated alteration exposed within a key section for understanding uranium mineralisation at the Four Mile West deposit. MESA J. 55, 34–39.
Hou, B., 2008. Palaeochannel studies related to the Harris Greenstone Belt, Gawler Craton, South Australia: Architecture and evolution of the Kingoonya Palaeochannel System. CRC LEME Open File Report 154. CRC LEME, Perth. 122 pp.
Hou, B., Mauger, A.J., 2005. How well does remote sensing aid palaeochannel identification? -an example from the Harris Greenstone Belt, SA. MESA J. 38, 46–52.
Hou, B., Frakes, L.A., Alley, N.F., 2001. Development of geoscientific models for exploration in Tertiary palaeochannels draining the Gawler Craton, SA: South Australia. Department of Primary Industries and Resources. Report Book, 2001/21.
Hou, B., Frakes, L.A., Alley, N.F., Clarke, D.A., 2003. Characteristics and evolution of the Tertiary palaeochannels in the NW Gawler Craton, South Australia. Aust. J. Earth Sci. 50, 215–230.
Hou, B., Alley, N.F., Gray, D.J., 2004. 3D palaeochannel modelling as an aid to exploration in palaeodrainage terrains - Harris Greenstone Belt, Gawler Craton, SA. In: McPhie, J., McGoldrick, P. (Eds.), Dynamic Earth 2004: Past, present and future: 17th Australian Geological Convention 2004, Abstracts v. 73. Geological Society of Australia, p. 21.
Hou, B., Fabris, A.J., Keeling, J.L., Fairclough, M.C., 2006. Palaeochannel uranium signatures and exploration models, southern Australia: The Australian Earth Sciences Convention 2006, Melbourne, 2–6 July 2006, 4pp.
Hou, B., Zang, W., Fabris, A., Keeling, J., Stoian, L., Fairclough, M., 2007a. Palaeodrainage and Tertiary Coastal Barriers of South Australia, Digital Geological Map of South Australia, 1:2 000 000 Series (1st Edition) (compilers). CRC LEME and Geological Survey of South Australia.
Hou, B., Fabris, A.J., Keeling, J.L., Fairclough, M.C., 2007. Cenozoic palaeochannel-hosted uranium and current exploration methods, South Australia. MESA J. 46, 34–39.
Hou, B., Frakes, L.A., Sandiford, M., Worrall, L., Keeling, J., Alley, N.F., 2008. Cenozoic Eucla Basin and associated palaeovalleys, southern Australia – climatic and tectonic influences on landscape evolution, sedimentation and heavy mineral accumulation. Sediment. Geol. 203, 112–130.
Hou, B., Keeling, J., Reid, A.J., Warland, I., Belousova, E., Frakes, L.A., Hocking, R., Fairclough, M., 2011. Heavy mineral sands in the Eucla Basin, southern Australia: deposition and province-scale prospectivity. Econ. Geol. 106, 687–712.
Hou, B., Fabris, A., Michaelsen, B., Katona, L., Keeling, J., Stoian, L., Wilson, T., Fairclough, M., Zang, W., 2012. Palaeodrainage and Cenozoic Coastal Barriers of South Australia. Digital Geological Map of South Australia, 1:2 000 000 Series (2nd Edition) (compilers). Geological Survey of South Australia, Adelaide.
Hou, B., Michaelsen, B., Li, Z., Keeling, J.L., Fabris, J.A., 2014. The participants of IGCP-514, Paleovalley-related uranium: exploration criteria and case-studies from Australia and China. Episodes 37 (3), 150–171.

Hou, B., Keeling, J., Van Gosen, B.S., 2017. Geological and exploration models of beach placer deposits, integrated from case-studies of southern Australia. Ore Geol. Rev. 80, 437–459.
Huang, X.F., Liu, D.C., Du, L.T., Zhao, Y.J., 2005. A new sandstone type uranium metallogenetic type—'structure—oil, gas type', in Jingwen, M. & Bierlein, F.P. (Eds.), Mineral Deposit Research: Meeting the Global Challenge: Proceedings of the Eighth Biennial SGA meeting, Beijing, China, August 2005, pp. 265–268.
IAEA, 2009. World Distribution of Uranium Deposits (UDEPO) With Uranium Deposit Classification: Iaea-TECDOC-1629. International Atomic Energy Agency, Vienna.
Inwood, N., 2009. Mulga Rock deposits January 2009 resource estimate. Coffey Mining Pty Ltd.
Jagodzinski, E.A., Fricke, C.E., 2010. Compilation of new SHRIMP U-Pb geochronological data for the southern Curnamona Province, South Australia, 2010. Department of Primary Industries and Resources. Report Book 2010/00014.
Jaireth, S., McKay, A., Lambert, I., 2008. Association of large sandstone uranium deposits with hydrocarbons -The geology of uranium deposits in Kazakhstan points to similar deposits in Australia. Geoscience Australia AusGEO News 89, 1–6.
Jaireth, S., Roach, I.C., Bastrakov, E., Liu, S., 2015. Basin-related uranium mineral systems in Australia: a review of critical features. Ore Geol. Rev. 76, 360–394.
Johnstone, S., 2013. Four Mile mineral resource - compliance with JORC code 2012. Alliance Resources Ltd. ASX Release, 20 December 2013.
Karner, K., Becker, E., 2009. Geological setting of the Langer Heinrich uranium mine, Namibia. In: AusIMM International Uranium Conference 2009. AusIMM, Darwin, pp. 97–98.
Kyser, K., Cuney, M., 2009. Unconformity-related uranium deposits. In: Cuney, M., Kyser, K. (Eds.), Recent and Not-So-Recent Developments in Uranium Deposits and Implications for Exploration. Mineralogical Association of Canada and Society for Geology Applied to Mineral Deposits, Quebec, pp. 161–219.
Lally, J.H., Bajwah, Z.U., 2006. Uranium deposits of the Northern Territory. Northern Territory Geological Survey Report, p. 87.
Lambert, I., Jaireth, S., McKay, A., Meizitis, Y., 2005. Why Australia has so much uranium. AUSGEO News 80, 7–10.
Li, H., Kuang, W., 2010. Metallogenesis and metallogenic model of the Nuheting uranium deposit in Erlian Basin. World Nuclear Geosci. 27–3, 125–129 (in Chinese with English abstract).
Li, Z.Y., Chen, A.P., Fang, X.H., Xia, Y.L., Jiao, Y.Q., Zhang, K., Xiao, X.J., Sun, Y., 2005. Metallogenetic conditions and exploration criteria of Dongsheng sandstone type uranium deposit in Inner Mongolia, China. In: Mao, J.W., Bierlein, F.B. (Eds.), Mineral Deposit Research: Berlin. Springer, pp. 291–294.
Li, H.T., Cai, C.F., Luo, X.R., Sun, X.Y., 2007. Geochemical evidence for sedimentary Province of Middle Jurassic sandstones in Dongsheng Area, Inner Mongolia. Chin. J. Geol. 42, 353–361.
Li, Z.Y., Fang, X.H., Chen, A.P., Ou G.X., Xiao, X.J., Sun, Y., Liu, C.Y., Wang, Y., 2007b. Origin of grey-green sandstone in ore bed of sandstone type uranium deposit in North Ordos Basin: Science in China (Series D): Earth Science, 50 (Suppl. II), Beijing Science in China Press, pp. 165–173.
Li, Z.Y., Chen, A.P., Fang, X.H., Ou, G.X., Xia, Y.L., Sun, Y., 2008. Origin and superposition metallogenic model of the sandstone-type uranium deposit in the northeastern Ordos Basin. China. Acta Geologica Sinica 82 (4), 745–749.
Liu, H., Xia, Y., Tian, S., 2007. Geochronological and source studies of uranium mineralization in Dongsheng. Uranium Geol. 23, 23–29.
Ludwig, K.R., Cooper, J.A., 1984. Geochronology of Precambrian granites and associated U-Ti–Th mineralisation, northern Olary Province, South Australia. Contrib. Miner. Petrol. 86, 298–308.
Luo, X., Taofa, Z., Hou, B., 2004. The geoelectrochemical extraction method (CHIM) in exploration for concealed ore deposits. In: Roach, I.C. (Ed.), Regolith 2004. CRC LEME, Perth, pp. 230–233.
Luo, X., Hou, B., Keeling, J.L., Fidler, R., Fabris, A.J., Zeng, N., Wen, M., 2006. CHIM-geoelectrochemical method in exploring for concealed mineralisation in China and Australia: 12th IAGOD Symposium, Moscow, 21–25 August 2006, pp. 11 (abstract), 4pp (short paper).
Macfarlane, I., Inwood, N., 2010. Mulga Rock deposits June 2010 resource estimate. Coffey Mining Pty Ltd.
Mann, A.W., Deutscher, R.L., 1978. Genesis principles for the precipitation of carnotite in calcrete drainages in Western Australia. Econ. Geol. 731, 1724–1737.
Mann, A.W., Horowitz, R.C., 1979. Groundwater calcrete deposits in Australia some observations from Western Australia. Aust. J. Earth Sci. 26, 293–303.
Marsland-Smith, A., Huddleston, A., Packer, B., Smith, A., 2011. Uranium exploration and recently discovered uranium deposits in the Frome Embayment, South Australia. In: Forbes, C.J. (Ed.), 2011 Sprigg Symposium, Abstracts 100. Geological Society of Australia, pp. 43–46.
McConachy, G., 2009, Pepegoona deposit, northern Flinders Ranges, SA: SA Explorer's Conference, Adelaide, 27 November 2009.
McKay, A., Miezitis, Y., 2001. Australia's Uranium: Resources, Geology and Development of Deposits: Mineral Resource Report 1. Geoscience Australia, Canberra.
Meng, Q.R., Hu, J.M., Jin, J.Q., Zhang, Y., Xu, D.F., 2003. Tectonics of the late Mesozoic wide extensional basin system in the China-Mongolia border region. Basin Res. 15, 397–415.
Michaelsen, B.H., Fabris, A.J., 2011. Organic facies of the Frome Embayment and Callabonna Subbasin: what are the U reductants? In: Forbes, C.J. (Ed.), 2011 Sprigg Symposium: Unravelling the northern Flinders and beyond, Abstracts No. 100. Geological Society of Australia, Adelaide, pp. 49–52.
Michaelsen, B.H., Fabris, A.J., 2014. Organic facies of the Frome Embayment and Callabonna Subbasin, South Australia: What and where the uranium reductants. Presentation at the AusIMM Uranium 2014 Conference, 10–14 June 2014, Perth.
Michaelsen, B.H., Marsland-Smith, A.B., Magarey, P.D., Fabris, A.J., Roach, I.C., Dhu, T., Katona, L.F., Keeling, J.L., 2012. Mapping basin architecture and salinity: A TEMPEST™ AEM interpretation of the Poontana Trough, northwestern Lake Frome region, in: Roach I.C. (Ed.), The Frome airborne electromagnetic survey, South Australia: implications for energy, minerals and regional geology, Geoscience Australia Record 2012/40 - DMITRE Report Book 2012/003.
Michaelsen, B.H., Fabris, A.J., Keeling, J.L., McKirdy, D.M., Katona, L.F., Tucker, L.R., 2016. Organic facies of the Frome Embayment and Callabonna Sub-basin: what and where are the uranium reductants? MESA J. 81, 35–65.
Min, M.Z., Luo, X.Z., Mao, S.L., Wang, Z.Q., Wang, R.C., Qin, L.F., Tan, X.L., 2001. An excellent fossilized wood cell texture with primary uranium minerals at a sandstone-hosted roll-type uranium deposit, NW China. Ore Geol. Rev. 17, 233–239.
Min, M.Z., Chen, J., Wang, J.P., Wei, G.H., Fayek, M., 2005. Mineral paragenesis and textures associated with sandstone-hosted roll-front uranium deposits, NW China. Ore Geol. Rev. 26, 51–69.
Min, M.Z., Xu, M.H., Chen, J., Fayek, M., 2005. Evidence of uranium biomineralization in sandstone-hosted roll-front uranium deposits, northwestern China. Ore Geol. Rev. 26, 198–206.
Murphy, M.J., Dosseto, A., Turner, S.P., Schaefer, B.F., 2011. U-Series disequilibrium in groundwater as a vector for U mineralisation. Mineral. Mag. 75, 1516.
Nash, J.T., Grainger, H.C., Adams, S.S., 1981. Geology and concepts of genesis of important types of uranium deposits. In: Skinner, B.J. (Ed.), Economic Geology Seventy-Fifth Anniversary Volume 1905–1980: El Paso. The Economic Geology Publishing Company, Texas, pp. 63–116.
Nie, F., 2008. Uranium mineralization of the Bayawula deposit, Erlian basin, northeast China: IAEA Technical meeting "Uranium exploration and mining methods", Jordan, Amman, Proceedings.
Nie, F., Chen, A., Hu, Q., Shen, K., Qin, M., Li, M., Jiang, M., 2007. Discussion on the early Cretaceous sandstone-type uranium deposits, Erlian Basin, Inner Mongolia. J. Stratigr. 31–3, 272–279 (in Chinese with English abstract).
OECD/NEA and IAEA, 2000. Uranium 2000: Resources, Production and Demand. OECD Nuclear Energy Agency, Paris.
OECD-NEA, IAEA, 2010. Uranium 2009: Resources, Production and Demand. OECD Nuclear Energy Agency, Paris.
OECD-NEA, IAEA, 2014. Uranium 2014: Resources, Production and Demand. OECD Nuclear Energy Agency, Paris.
Otton, J.K., 1984. Surficial uranium deposits: summary and conclusions. Surficial Uranium Deposits. IAEA, Vienna. IAEA-TEDOC-322 (252 pp.).
Pan, S., Wei, P., Wang, T., et al., 2011. Discovery of provenance in eastern part of Songliao Basin and its significance of oil geology. Nat. Gas Geosci. 22 (6), 1021–1027 (in Chinese).
Pechenkin, I., 2014. Sandstone uranium deposits of Eurasia: from genetic concepts to forecasting new discoveries. In: URAM 2014. IAEA, Vienna, p. 68.
Penney, R., 2012. Australian sandstone-hosted uranium deposits – a review. IMM Appl. Earth Sci. 121 (2), 65–75.
Reif, T., 2000. Honeymoon uranium project update. MESA J. 19, 4–7.
Reynolds, R.L., Goldhaber, M.B., 1978. Origin of a South Texas roll-type uranium deposit; I, Alteration of iron-titanium oxide minerals. Econ. Geol. Bull. Soc. Econ. Geol. 73, 1677–1689.
Roach, I.C., Jaireth, S., Costelloe, M.T., 2014. Applying regional airborne electromagnetic (AEM) surveying to understand the architecture of sandstone-hosted uranium mineral systems in the Callabonna Sub-basin, Lake Frome region, South Australia. Aust. J. Earth Sci. 61, 659–688.
Sanford, R.F., 1994. A quantitative model of ground-water flow during formation of tabular sandstone uranium deposits. Econ. Geol. 89 (1,2), 341–360.
Schofield, A., 2009. Uranium Content of Igneous Rocks of Australia 1:5000000 Maps -Explanatory Notes and Discussion. Geoscience Australia, Canberra.
Schmid, S., Foss, C., Hill, J., Quigley, M., Schaubs, P., Cleverley, J., Robinson, J., 2012. JSU Ngalia Basin Uranium Mineral System Project. In: Munson, T.J., Johnston, K.J. (Eds.), Geological Survey Record 2012–003. Northern Territory Geological Survey, Darwin, Northern Territory, Australia, pp. 60–62.
Schumm, S.A., 1981. Evolution and response of the fluvial system: sedimentologic implications. In: Ethridge, F.G., Flores, R.M. (Eds.), Recent and Ancient Nonmarine Depositional Environments: Models for Exploration. Society of Economic Paleontologists and Mineralogists, Special Publication, 31, pp. 19–29.
Shi, T., Cheng, J., Xie, X., et al., 2012. Water isotopic characteristics and geological significance of the western Songliao Basin. J. Sedimentol. 20 (2), 399–404 (in Chinese).
Skirrow, R.G., 2009, (Ed.), Uranium ore-forming systems of the Lake Frome region, South Australia: Regional spatial controls and exploration criteria. Geoscience Australia Record 2009/40, 151p.
Southern Cross Resources Australia Pty Ltd, 2000. Honeymoon Uranium Project Environmental Impact Statement. Toowong, Queensland, Southern Cross Resources Australia Pty Ltd.
Spirakis, C.S., 1996. The roles of organic matter in the formation of uranium deposits in sedimentary rocks. Ore Geol. Rev. 11, 53–69.
Stoian, L.M., 2010. Palynology of Mesozoic and Cenozoic sediments of the Eromanga and Lake Eyre basins: results from recent drilling in the northwest Frome Embayment. MESA J. 57, 27–35. Primary Industries and Resources South Australia, Adelaide.

Sun, Y., Liu, C., Lin, M., Li, Y., Qin, P., 2009. Geochemical evidences of natural gas migration and releasing in the Ordos Basin, China. Energy Explor. Exploit. 27, 1–13.
Thundelarra Exploration Ltd., 2012. Ngalia Basin uranium project: Bringing Forward Discovery, Northern Territory Mineral Investment Opportunities, June 2012, Northern Territory Geological Survey, www.bfd.nt.gov.au.
Tonkin, D., 2009. Curnamona Province exploration review and mineral systems. Department of Primary Industries and Resources, South Australia. Report Book 2009/10.
Uranium One, 2007. Honeymoon project, Mineral Lease 6109. Mining and Rehabilitation Program. Uranium One.
Uranium, S.A., 2013. Activities report 3 months ended 30 September 2013. Uranium SA Ltd. ASX Release 28 October 2013.
Wade, C.E., 2011. Definition of the Mesoproterozoic Ninnerie Supersuite, Curnamona Province, South Australia. MESA J. 62, 25–42.
Wei, S., Qin, M., Li, Y., He, Z., Chen, A., Shen, K., 2005. Late Mesozoic-Cenozoic tectonosedimentary evolution and sandstone-hosted uranium mineralization of the Erlian basin. 8th Biennial SGA Meeting Beijing, Metallogeny and Exploration. Mineral Deposit Research: Meeting the Global Challenge, pp. 320–322 (Chapter 3–27).
Wilford, J., Worrall, L., Minty, B., 2009. Radiometric map of Australia provides new insights into uranium prospectivity, AUSGEO News 95, Canberra, Geoscience Australia, pp. 1–4.
Wilson, T., 2015. Uranium and Uranium Mineral Systems in South Australia – Third Edition, Report Book 2015/00011. Department of State Development, South Australia, Adelaide.
Wülser, P.A., Brugger, J., Foden, J., Pfeifer, H.R., 2011. The sandstone-hosted Beverley uranium deposit, Lake Frome Basin, South Australia: Mineralogy, geochemistry, and a time-constrained model for its genesis. Econ. Geol. 106, 835–867.
Xia, Y., Lin, J., Liu, H., 2003. Geochronological studies of sandstone-type uranium deposits in major uranium-producing basins in northern China. Uranium Geol. 19, 129–136 (in Chinese with English abstract).
Xia, Y.L., Lin, J.R., Liu, H.B., Fan, G., Hou, Y., 2003. Research on geochronology and sandstone-hosted uranium ore formation in major uranium productive basins, northern China. Uranium Geol. 19 (3), 129–136 (in Chinese).
Xue, C., Chi, G., Wei Xue, W., 2010. Interaction of two fluid systems in the formation of sandstone-hosted uranium deposits in the Ordos Basin: geochemical evidence and hydrodynamic modelling. J. Geochem. Explor. 106, 226–235.
Yan, Y., An, W., Xu, X., 2010. Study on Rocks Feature in Ore Target Layers of Nuheting Mudstone-type Uranium Deposit, 4. China Acad. J. Publishing House, pp. 44–46.
Zhang, J., Li, Z., 2008. Uranium potential and regional metallogeny in China. Acta Geol. Sinica 82 (4), 741–744.
Zhang, L.P., Bai, G.P., Zhao, K.B., Sun, C.Q., 2006. Restudy of acid-extractable hydrocarbon data from surface geochemical survey in the Yimeng Uplift of the Ordos Basin, China: improvement of geochemical prospecting for hydrocarbons. Mar. Petrol. Geol. 23, 529–542.